To the Graduate Council:

I am submitting herewith a thesis written by Christopher Lee Whitten entitled "Development of a Ground-Based Remote Sensing System with Modulated Illumination for Diagnosing Nitrogen Status in Cotton." I have examined the final electronic copy of this thesis for form and content and recommend that it be accepted in partial fulfillment of the requirements for the degree of Master of Science, with a major in Biosystems Engineering.

John B. Wilkerson

Major Professor

We have read this thesis and
recommend its acceptance:

Luther R. Wilhelm

J. Wesley Hines

Accepted for the Council:

Anne Mayhew

Vice Provost and
Dean of the Graduate Studies

(Original signatures are on file in the graduate student services office.)

DEVELOPMENT OF A GROUND-BASED REMOTE SENSING SYSTEM WITH MODULATED ILLUMINATION FOR DIAGNOSING NITROGEN STATUS IN COTTON

A Thesis

Presented for the

Master of Science

Degree

The University of Tennessee, Knoxville

Christopher Lee Whitten

May 2002

DEDICATION

This thesis is dedicated to my wife, Alicia. Without her endless love, understanding and support, this work would not have been possible.

ACKNOWLEDGMENTS

The author wishes to express his sincere appreciation to Dr. John B. Wilkerson, who served as his major professor, for his friendship, patience, and guidance. Appreciation is also extended to committee members, Dr. Wesley Hines and Dr. Luther Wilhelm for their support. Thanks are also extended to Henry Moody for his support, guidance, mentorship, and friendship. Special thanks are extended to Newman Webb, John Hancock, Eric Simmons, Seth Rye, and Will Pinson for their friendship and support.

Appreciation is extended to David Smith, Craig Wagnor, and Walker Garner for assistance in construction of prototypes. Sincere appreciation is also expressed to the Jackson Agricultural Experiment Station staff for their assistance in field experiments.

Most importantly, the author wishes to thank God for His gift of salvation through His Son, Jesus Christ.

ABSTRACT

Cotton production efficiency has the potential to increase through accurate variable rate application of fertilizer. The ability to variably apply fertilizer already exists. However, an accurate real-time system capable of diagnosing fertilizer deficiencies has yet to be implemented. A ground-based remote sensing system with modulated illumination has been developed for diagnosing nitrogen status in cotton plants. Development of the system was in part based on recommendations from previous research conducted at The University of Tennessee. The prototyped system consists of a multi-spectral sensing unit, a data acquisition and processing unit, and a graphical user interface. The multi-spectral sensing unit utilizes a discriminating artificial illumination source to eliminate error associated with the use of sunlight. Solar angle and atmospheric filtering contribute to variability in light intensity. Narrow spectrum ultra bright LEDs (blue, green, red, and infrared) with peak wavelengths of 466, 540, 644, and 880 nm were used. Modulated light at a frequency of 18.9 kHz was focused into a scanning beam and reflected from the plant canopy. Reflected light from the plant canopy was converted to voltage signals representing reflected light intensity at each waveband. A band pass filter was implemented to pass only the signal due to the modulated light source. The data acquisition and processing system was developed for control of the multi-spectral sensing unit and reliable data collection and processing. The prototyped system was tested on DP451 BRR cotton with four different N application rates. Based on a nitrate analysis, three nitrogen status classifications were identified: low, medium, and high. Analysis of spectral data collected revealed reflected light energy in the red region produced the highest linear correlation with N status ($r = -0.7285$).

A feed forward neural network was trained to predict nitrogen status based on the four spectral measurements taken with the prototyped system. System performance was evaluated based on its ability to correctly classify N status. Results indicate that the system is capable of diagnosing nitrogen status in cotton with a high degree of accuracy. Using dynamically (≈1 mi/hr) acquired data, prediction accuracies as high as 91% were achieved when 50% of data was used for training and 50% used for testing. Accuracy decreased slightly to 90% when 25% of the data was used for training and 75% used for testing. Utilizing neural networks, the prototyped system outperformed the conventional NDVI and other linear techniques. The system has shown great potential in diagnosing N status in cotton under controlled field conditions. Future testing should be performed to evaluate the system for multiple varieties, growing seasons, and other variables known to contribute to plant health variability.

TABLE OF CONTENTS

Chapter *Page*

Chapter 1 *CHAPTER I. INTRODUCTION* *1*

Justification for Research **1**

Objectives **2**

Chapter 2 *CHAPTER II. REVIEW OF LITERATURE* *4*

Plant Spectral Reflectance Characteristics **4**

Plant Discrimination with Spectral Reflectance **5**

Spectral Reflectance Sensors for Plant Health **7**

Spectral Reflectance measurements in cotton **9**

Analytical Techniques **10**

Vegetative Indices 10

Artificial Neural Networks 11

Chapter 3 *CHAPTER III. METHODS AND MATERIALS* *15*

Background **15**

System Overview **16**

Multi-Spectral Sensing Unit Design **18**

Design Overview 18

Emitter Design 19

Overview 19

Optical System 19

Electronic System 22

Emitter Sub-Assembly Mounting 26

Detector Design 29

Overview 29

Optical Sub-System 29

Optoelectric Interface 32

Detector Sub-Assembly Mounting 32

Data Acquisition and Processing System Design **35**

Hardware 35

Overview 35

Single-board Computer 36

Graphical User Interface 36

Power Requirements 36

Software for Data Acquisition and Processing 37

Data Acquisition Program 37

Neural Network 39
Testing Procedures 39
Experimental Plot Layout 39
Spectral Data Acquisition 40
Ground Truthing of Experimental Data 41
Plant Nitrogen Measurements 41
Plant Nitrate Analysis 41
Neural Network Training and Testing 42
Data Post-Processing 44
Chapter 4 *CHAPTER IV. RESULTS 46*
Spectral Band Correlations with N Status 46
Neural Network 48
Linear regression 52
NDVI Index 52
Summary 54
Chapter 5 *CHAPTER V. SUMMARY AND CONCLUSIONS 57*
Summary 57
Conclusions 58
Recommendations 59
System Refinements 59
Additional Testing 59
Chapter 6 *BIBLIOGRAPHY 61*
Chapter 7 *APPENDICIES 65*
Appendix A Mechanical Drawings 66
Appendix B Electronic Device Specifications 68
Appendix C Data Acquisition Program 80
Appendix D Matlab Post-Processing Programs 86
VITA 98

LIST OF TABLES

Number ***Page***

Table 1. Data percentages used for training and testing. 44

Table 2. Correlation coefficients matrix created from dynamically acquired data. 47

Table 3. Correlation coefficients matrix created from statically acquired data. 47

Table 4. Summary of results with decision made every scan. 51

Table 5. Summary of results with decision made based on a majority rule using ten scans. 51

Table 6. Neural Network prediction error matrix. 56

Table 7. Regression model prediction error matrix. 56

Table 8. NDVI model prediction error matrix. 56

LIST OF FIGURES

Number ***Page***

Figure 1. Significant spectral response characteristics of green vegetation (Swain and Davis, 1978). 5

Figure 2. Example of MLP architecture. 13

Figure 3. Block diagram of prototype system. 17

Figure 4. Concept of multi-spectral sensing unit. 19

Figure 5. LEDs are aligned in a single array and light cones are collimated in one dimension to create a linear scanning beam. 21

Figure 6. Portions of the LEDs were removed leaving an angle of 0.5 degrees on both sides of each modified LED. 23

Figure 7. Centerline of all LEDs are directed toward a single point ten inches from the LED array. 24

Figure 8. Fabricated prototype emitter assembly. 25

Figure 9. Emitter Board Circuit Schematic. 27

Figure 10. Sensing Unit with panel removed to reveal the detector and emitter sections. 28

Figure 11. Photodiode soldered to PCB. 30

Figure 12. Lens holder mounted securely over the photodiode. 30

Figure 13. LED luminous intensities (1-blue, 2-green, 3-red, 4-NIR) and photodiode response (5). 31

Figure 14. Optoelectric interface Board Circuit Schematic. 33

Figure 15. Measured band pass filter (with gain) response to a one-volt sine wave. 34

Figure 16. Photodiode and LED array orientation.....34

Figure 17. Data Acquistion and Processing schematic.....35

Figure 18. Flow diagram of Visual Basic Data Acquisition Program. 38

Figure 19. Nitrate measurements in ppm as a function of nitrogen application rate.....43

Figure 20. Example of soil at end of crop row. 45

Figure 21. Optimum network architecture for diagnosing nitrogen status. 48

Figure 22. Three classification categories for N status.....49

Figure 23. Regression prediction and thresholds for dynamically collected data with 50% for training and 50% for testing (scenario 1).....53

Figure 24. Average NDVI as a function of Nitrate (ppm). 55

Figure 25. Average NDVI as a function of N application rate.....55

CHAPTER I. INTRODUCTION

Justification for Research

Agricultural practices have become more sophisticated with the passing of each decade. In the last century, acreage per farm has grown tremendously in part due to the advent of large farm machinery. Advances in agricultural related technology have exploded in the past decades and will continue to grow in the 21st century. New chemicals, machinery, electronics, and crop varieties have led to huge increases in production efficiency. As part of the crop production technology expansion, the group of products and practices commonly clustered under the umbrella term "precision farming" is becoming more and more accepted and may soon be vital to farm profit margins. A prime example of a precision farming practice is variable rate application of nitrogen (N) fertilizer. It is well known that optimum N application can maximize yields. More importantly, optimization of N application can maximize profits while potentially minimizing negative environmental impacts.

Cotton is an important crop world wide and one of the most researched. As with other crops, N is essential for healthy cotton plants and maximum cotton yield. Precision farming technology currently provides control systems with the ability to variably apply N. However, research is ongoing to find a quick, reliable, and inexpensive method for measuring plant stress due to nitrogen deficiencies. The need exists for an inexpensive real-time ground-based remote sensing system capable of estimating site-specific N application rates.

Research has shown cotton plant canopies with different N concentration levels have different spectral characteristics (Sui, 1999). Therefore, a multi-spectral sensing system with the ability to be trained to recognize unique spectral signatures could be used to provide the real-time inputs for variable rate application of N. During previous research at The University of Tennessee, Sui (1999) developed a first generation multi-spectral sensor. Sui's ground-based remote sensing system with Artificial Neural Networks (ANN) has shown great potential for real-time variable-rate control of N in cotton. With the output of Sui's sensor, ANNs were able to learn non-linear relationships between reflected light characteristics of cotton and N content. Utilizing some valuable suggestions, it would be advantageous to build on Sui's research by designing an improved, inexpensive, and compact system for diagnosing N status in cotton.

Objectives

The goal of this study was to design, fabricate, and test a prototype real-time ground-based multi-spectral sensing system capable of being trained to recognize various levels of nitrogen deficiency in cotton plants. To achieve this goal, specific objectives were defined as follows:

1. Design and fabricate a prototype multi-spectral sensing unit with an illumination source that is independent of natural illumination.
2. Develop a system for data acquisition and processing of sensing unit output to recognize nitrogen deficiencies.
3. Analyze linear relationships between N and reflected light measurements taken with the prototype sensor.

4. Train and test an artificial neural network for predicting nitrogen status in cotton.

CHAPTER II. REVIEW OF LITERATURE

Plant Spectral Reflectance Characteristics

Spectral reflectance characteristics of healthy green plants are distinctive, having similar variations in light spectra. Figure 1 shows a typical reflectance curve for green vegetation and identifies major wavelength bands of significance. In the visible bands, chlorophyll plays a very significant role in plant pigmentation (Swain and Davis, 1978). It is well known that nitrogen is an essential element for healthy plant growth and chlorophyll synthesis (Borhan et al., 2001). Increasing nitrogen content has been shown to increase chlorophyll (Wood et al., 1992). Centered at 450 nm and 650 nm, two major bands of significance in the visible region are due to chlorophyll absorption. These bands fall in the blue and red regions of the visible spectrum. Between these two absorption bands, a peak reflectance centered at 540 nm is a distinctive characteristic of healthy plants. With this peak falling in the green-wavelength region, it is the relatively low absorption here that causes healthy foliage to appear green to the human eye (Swain and Davis, 1978). Since nitrogen plays a role in chlorophyll synthesis, it can be concluded that nitrogen deficiencies affect plant spectral response in the visible spectrum. More importantly, it may be possible to extract useful spectral information from the three visible spectral regions discussed. Green plants absorb very little in the near infrared region accounting for the distinctive rise in reflectance. Although near infrared plant reflectance is not affected by the major absorption bands, it may be useful as a baseline for the visible reflectance intensity measurements. In the middle-infrared region, three water absorption bands dominate

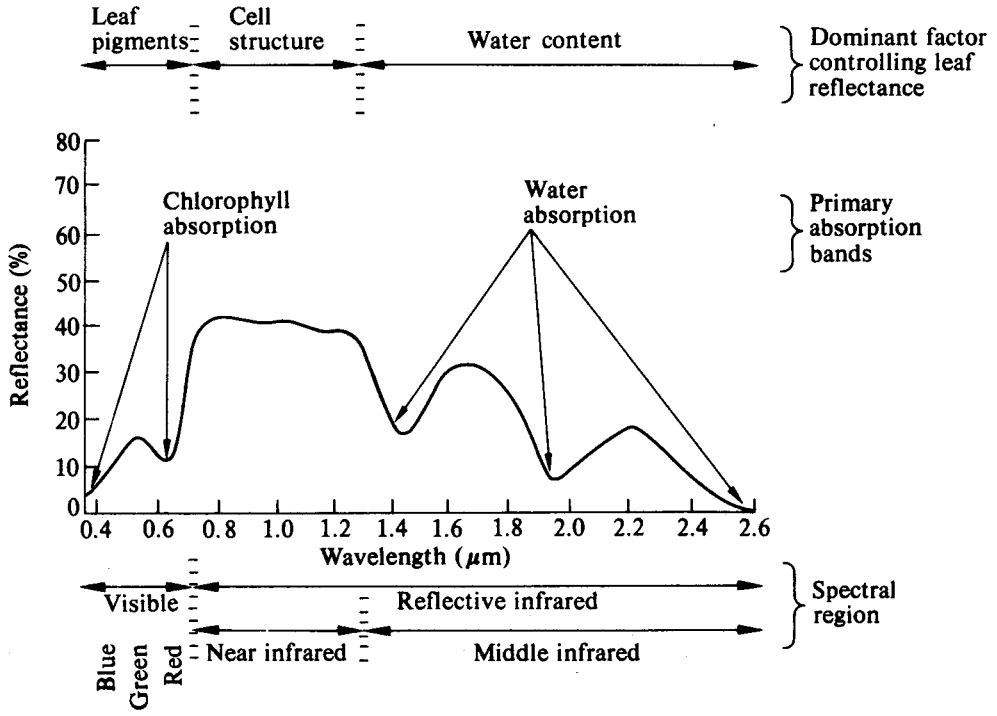


Figure 1. Significant spectral response characteristics of green vegetation (Swain and Davis, 1978).

spectral response characteristics. Reflectance from this region may be useful in measuring plant moisture content.

Plant Discrimination with Spectral Reflectance

Spectral reflectance characteristics of plants will vary depending on stress due to drought or nutrient deficiencies. Even more so, reflectance characteristics can vary from species to species and variety to variety. Scott and Trever (2001) used reflectance spectra

to discriminate six plant species, of which three were crops and three were weeds. Crops selected for this study were wheat, Argentine canola, and field peas. Weeds selected for this study were wild oats, wild buckwheat, and Canada thistle. Reflectance measurements were taken using a spectrophotometer at wavelengths ranging from 250 nm to 2500 nm with a resolution of one nanometer between 250 and 870 nm and two nanometers between 870 and 2500 nm. Data were then averaged to give a spectral bandwidth of 10 nm. Classifiers using fewer than five wavelength features successfully distinguished between the six species with accuracies greater than 90%. The study suggests successful wavelengths for this application are near 420 nm, 360 nm, 680 nm, and 1930 nm.

Beck and Vsye (1995) patented an apparatus and method for selective elimination of weeds in agricultural operations. Two light emitters with wavelengths in the red and near infrared region are modulated at high frequencies. On/off modulation of one emitter is approximately 90 degrees out of phase with the other. Light beams provided by the emitters are reflected off plant or soil. Reflected radiation is intercepted by a photodiode. The ratio of reflected radiation at the two wavelengths is converted to a phase. Phase information is used to detect the presence of a plant. This apparatus and method requires a calibration step that may introduce problems. Kinter and Beck (1998) patented an apparatus and method that eliminates the calibration step. For living plants, reflectance generally decreases from 600 to about 670 nm and increases from 670 to 700 nm. With three different wavelengths, change in slope of reflectance characteristic could be used to discriminate between plants and soil.

Spectral Reflectance Sensors for Plant Health

An accurate (non-intrusive) method of measuring plant chlorophyll could provide useful information relating to nitrogen application rates of crops. The Soil-Plant Analyses Development (SPAD) division of the Minolta Camera Company has developed a unit to measure chlorophyll in a plant leaf. Krugh et al. (2000) provides a brief description of the SPAD-502 Minolta chlorophyll meter. The meter utilizes two light emitting diodes (LEDs), a red LED with a peak wavelength of 650 nm and an infrared LED with a peak wavelength of 940 nm. LED light enters the leaf where a portion of the light is absorbed by chlorophyll and the remainder is transmitted through the leaf where a silicon photodiode detector converts it into an electrical signal. This electrical signal is inversely proportional to the amount of chlorophyll in the light path. After the signal processing, absorbance is displayed in arbitrary units from 0 to 199. Measurements take only seconds to perform and the meter is equipped to store 30 readings, average the data, and make data deletions when necessary. Since measurements are in arbitrary units, only relative comparisons can be made. To make measurements useful and meaningful, data can be correlated to actual amounts of chlorophyll. Note that this hand-held unit is intrusive. The meter is "clamped" such that the light and the detector are on opposite sides of the leaf.

Borhan et al. (2001) used multi-spectral imaging techniques to predict chlorophyll and nitrogen status of potato leaves. Plots were established with five different application levels of ammonium nitrate. An image acquisition system consisting of a Hitachi CCD color video camera and two 50 W tungsten halogen lamps was used to acquire RGB images. Immediately after image acquisitions, nitrate and chlorophyll content were determined in the laboratory. From the RGB color images, four image features were

extracted for a chlorophyll prediction model. The correlation coefficient between actual and predicted chlorophyll was 0.8032.

Research at The University of Tennessee has led to the development of a plant health sensor (Sui, 1999). A multi-spectral plant health sensor was developed and field tested. The sensor detects a reflected light energy in four wavebands (blue, green, red and near infrared). To eliminate error due to variations in sunlight intensity, a modulated broad band artificial light source was used to illuminate the plant canopy. Two halogen bulbs modulated at 60 Hz served as the artificial illumination source. Optical filters passed the wavebands of interest while blocking all other wavelengths of light. Sunlight and artificial light energy within the passing wavelength ranges (350-500 nm, 520-580 nm, 600-740 nm, and 750-1100 nm) were focused onto four photodiodes. From each photodiode, plant canopy reflected light for each band was converted to a voltage signal. A band-pass filter was used to pass the modulated light energy while attenuating frequencies outside the band. The sensor used four demodulation circuits to obtain analog DC voltage signals representing the reflectance in each of the four wavelength ranges.

Stone et al. (2001) developed optical based sensors for detection of N availability in winter wheat. The sensor measured reflectance in three different wavebands (green, red, and NIR). Three photo detectors along with interference filters were used to achieve reflectance measurements of wavelengths centered at 550±6, 671±6, and 780±6 nm (NIR). Reflectance was found to rise in the NIR band and fall in the red band for increasing N availability. Results show a strong correlation between spectral index and N mass. Stone addressed the concern of biomass correlation with spectral indices. Stone indicates that

total chlorophyll mass in vegetative material is the product of chlorophyll concentration and vegetative mass

Spectral Reflectance measurements in cotton

Sui (1999) documented the relationship between N status of cotton plants and spectral reflectance characteristics of the cotton canopy. Spectral reflectance measurements from the cotton canopy were taken with a SD-1000 Fiber Optic Spectrometer (Ocean Optics). The measured spectrum ranged from 237 to 816 nm. Cotton plots were established and N was applied at 0, 30, 60, 90, and 120 lbs per acre. Petioles were randomly collected from 10 plants within each plot. A nitrate content analysis was performed on the plant petioles. Yield measurements were also taken for each of the plots. Various variable selection techniques were used to select the best independent variables to explain variation in the dependent variable. A spectral index was developed which showed the highest correlation with petiole nitrate content, yield, and nitrogen application rate.

$$Spectral\ Index = (NIR + Blue) / (Green + Red)$$

Where

Blue: Normalized spectral reflectance from 460 to 490 nm;

Green: Normalized spectral reflectance from 545 to 565 nm;

Red: Normalized spectral reflectance from 600 to 610 nm;

NIR: Normalized spectral reflectance from 740 to 770 nm.

From this study, it was concluded that cotton leaves with different nitrogen concentration levels have different spectral reflectance characteristics.

Read et al. (2001) researched the effects of nitrogen stress on cotton canopy spectral reflectance and yield. This study found plant reflectance at 437 nm (blue) and 610 nm (red) to be closely related to leaf nitrogen. The ratio of blue to red at these wavelengths had an r^2 of 0.77 with leaf nitrogen. This was found to be the best two-waveband model for predicting leaf N concentration from canopy reflectance. The highest r^2 was 0.92 and came from the best seven-waveband model. Read et al. concludes that his results indicate reflectance ratios measured in spectrally narrow wavebands should improve significantly our capability to detect N status in cotton with imaging, as well as non-imaging systems.

Analytical Techniques

Vegetative Indices

Vegetative indices based on red and infrared reflectance have been used to recognize N deficiencies (Blackmer et al., 1996; Stone et al., 1997). One of the most commonly used vegetation indices is the normalized difference vegetation index (NDVI). NDVI is computed using the formula:

$$NDVI = \frac{IR - R}{IR + R}$$

Where

R = spectral reflectance in the red region;

IR = spectral reflectance in the infrared region.

Plant et al. (2000) researched spectral measurements based on NDVI and their usefulness for site-specific management of cotton. Although NDVI did not indicate the source of stress by itself, it was concluded that it could be a fairly good predictor of higher nitrogen deficiencies in cotton. But the study shows NDVI may not necessarily be an accurate predictor of cotton yield.

Research has brought about variations in vegetative indices. For instance, Wang et al., (2001) developed an optical weed sensor based on a study of spectral characteristics of weeds, wheat, and bare soil. Five feature wavelengths (496 nm, 546 nm, 614 nm, 676nm, and 752 nm) were identified and utilized in the design of the sensor. Five band pass color filters with peak wavelengths corresponding to the identified features were used. A color index was formed using the feature wavelengths in the form of normalized difference:

$$C = \frac{a_i - a_j}{a_i + a_j}$$

where a_i and a_j are light absorbances measured as feature wavelengths *i* and *j*, respectively. The *i-j* pairs used for four color indices were {614 nm, 546 nm}, {676 nm, 546 nm}, {676 nm, 496 nm}, and {752 nm, 676 nm}. Variations in illumination were found to have no significant effect on normalized color indices. Results from this study show classification rates of wheat, bare soil, and weeds to be 83.1%, 79.5%, and 62.5%, respectively.

Artificial Neural Networks

Artificial Neural Networks (ANNs) possess the ability to learn relationships in non-linear systems. Inspired by the parallel structure of the brain, an ANN consists of simple highly interconnected processing elements referred to as artificial neurons. The output of a standard artificial neuron is calculated by multiplying its inputs by a weight vector,

summing the results, and applying an activation function to the sum (Hines, 1997). Neurons make up layers within a neural network. Input layers are generally not included in specifying the number of layers in neural network architecture since they perform no real function other than providing inputs to the next layer. A network can contain multiple layers and is sometimes referred to as a multilayer perceptron (MLP). Layers placed between the input and output layers are referred to as hidden. An example of feed-forward MLP network architecture is graphically illustrated in figure 2. Feed-forward refers to a network with neuron connections flowing forward toward the output layer with no connections flowing backward or lateral. A neural network can be trained to approximate unknown functions by adjusting the gain (weights) placed on the connections between elements. Research has proven that a standard feed-forward MLP containing a single non-linear hidden layer can approximate any continuous function with any degree of accuracy over a compact set (Cybenko, 1989; Hornick, 1989; Funahashi, 1989). Haykin (1994) provides a comprehensive look at the research leading to this conclusion. For this reason, the MLP has been given the name "universal approximator".

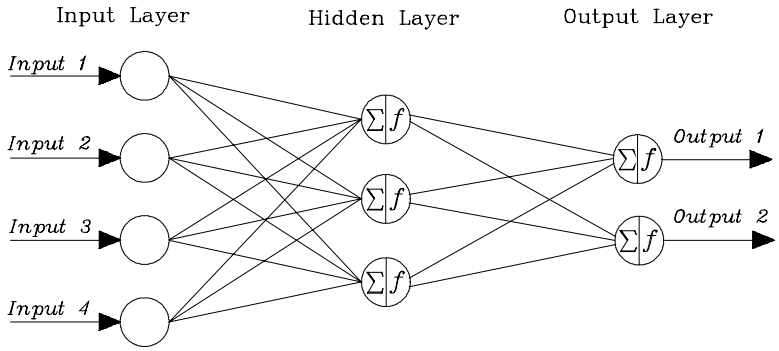


Figure 2. Example of MLP architecture.

Artificial neural networks have been used in a wide variety of applications where information extraction and real-time data processing are required. Sui (1999) used an artificial neural network to diagnose the nitrogen status in cotton plants. A network with five inputs, three neurons in the hidden layer, and two outputs was trained and tested with MATLAB®. The two outputs were nitrogen deficient or non-nitrogen deficient. With 50% of the data used for training and 50% using for testing, the neural network diagnosed the nitrogen status in cotton with accuracy greater than 95%. With 25% of the data used for training and 75% used for testing, accuracy still remained high at 87%.

Tumbo et al., (2001) utilized neural networks in an on-the-go system for sensing chlorophyll status in corn. A neural network was trained using a backpropagation

algorithm. A total of 201 inputs (spectral reflectance between 407 and 940 nm) were used in the training and testing of the neural network. Output for the network was SPAD units. A single hidden layer was used and contained 110 neurons. Neurons in the hidden and output layers used sigmoid logistic activation functions. At 0.37 mi/hr, the system predicted 86% of the chlorophyll readings within ±1 SPAD units. Less than desirable accuracy was achieved at higher speeds most likely due to less data used to predict chlorophyll readings.

Stone (1994) developed an ANN to use color patterns for weed recognition in an agricultural sprayer application. The sprayer system consisted of a three band optical sensor, a micro-controller, and a spray nozzle. The intent of the system was to detect weeds based on color and spray them. Training data were created with sensor output spanning all possible application conditions. A neural network model was trained and correctly recognized 92.5% of plants and 80% of no plant situations. The trained network was coded in C, compiled and used in the micro-controller. The prototype sprayer system was tested during the fall of 1993. Field test results indicated a loss of sensitivity under low light conditions. It was concluded that the developed ANN model performed within expectations while operating under conditions for which it was trained. Although, caution should be taken to insure that training of ANN models span all possible applications for the model.

CHAPTER III. METHODS AND MATERIALS

Background

Some background information is necessary to understand the design decisions that led to the development of the current prototype system. Previous work in the area of remote plant health sensing has been performed at The University of Tennessee. Sui (1999) developed two prototype plant health sensors (Models SL98 and AL98). Using optical filters in a four band sensor design, both models measured plant canopy reflectance in four spectral bands (350-500 nm, 520-580 nm, 600-740 nm, and 750-1100 nm). The first prototype (Model SL98) measured solar radiation reflected from the plant canopy. However, testing revealed that the reflected energy from sunlight varied with solar angle and atmospheric conditions. This led to the development of an artificial illumination that was used in conjunction with the second prototype (Model AL98). The second prototype was designed to measure only light energy originating from an artificial illumination source. To accomplish this, a broad band artificial illumination source was modulated at 60 Hz, and a demodulation circuit was added to the sensor's electronics. This filtered out the low frequency effects of solar radiation while passing the modulated frequency from the artificial light sources. Model AL98 was tested and successfully measured plant canopy reflectance originating only from the modulated illumination source.

Sui (1999) made valuable suggestions for the development of future sensor prototypes. One of the recommendations was to limit each spectral band to a narrower

wavelength range. This would increase the signal-to-noise ratio by limiting the measurement to light energy within the narrow waveband of interest.

A second recommendation involved the illumination source. Although the use of a broad spectrum modulated illumination source was successful, its implementation lacked efficiency. Two halogen bulbs were used in the design. LEDs have advantages over halogen bulbs such as low power consumption, compactness, and the capability of being modulated at much higher frequencies. Therefore, Sui (1999) recommended the use of modulated LEDs in future prototypes.

System Overview

The prototype system described in this thesis consists of three major sub-systems, (1) a data acquisition and processing (DAP) system, (2) a graphical user interface, and (3) a multi-spectral sensing unit (Figure 3.). A handheld PDA serves as the graphical user interface for the DAP processor via an ethernet connection. The DAP system outputs digital control signals to the sensing unit and receives analog signals representative of reflected light energy at four different wavelength bands of light. The sensing unit sequentially emits light in four wavebands and measures reflected light intensity from each band. The DAP system sequentially converts each analog signal to digital data. Acquired data can be stored for training of a neural network or processed in real-time using a trained neural network.

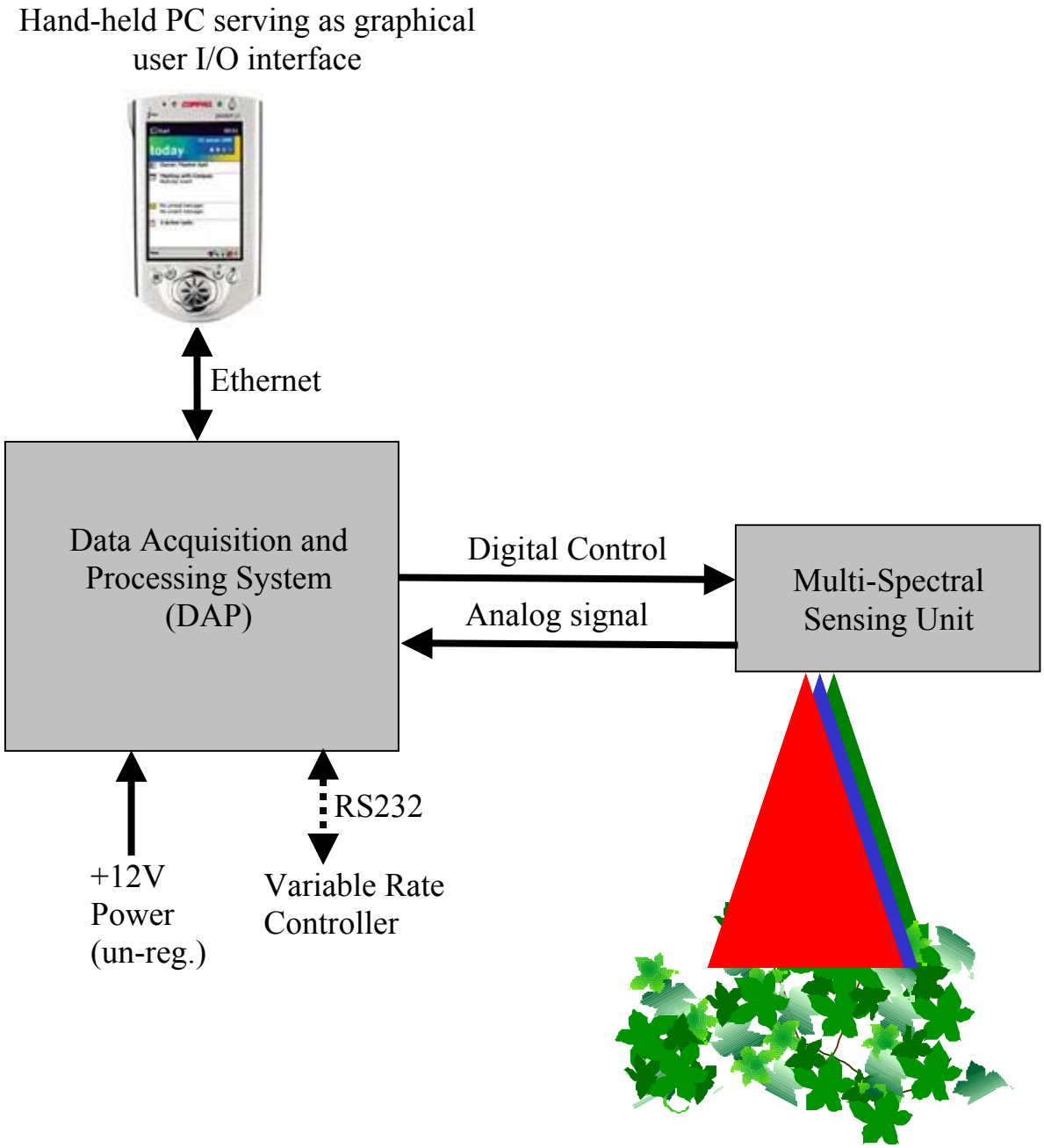


Figure 3. Block diagram of prototype system.

Multi-Spectral Sensing Unit Design

Design Overview

The first objective defined for this study was to design and fabricate a prototype multi-spectral sensing unit with a modulated illumination source. Design and development of a working prototype multi-spectral sensing unit was accomplished by defining sub-system design goals. Specific sub-system design goals are identified as follows:

1. Design and fabricate an illumination source capable of emitting and projecting modulated multi-spectral radiation bands onto a designated target.
2. Design and fabricate a sensor to detect only reflected modulated light from the plant canopy.
3. Integrate the light source, optics, and photo-electronics into a single sensing unit with light source and optics positioned for optimum performance.

As described in the system overview, the multi-spectral sensing unit must be capable of illuminating a target and measuring resulting light reflected from four wavebands: Blue, Red, Green, and Infrared. Such a prototype multi-spectral sensing unit has been designed and fabricated. The unit is comprised of two sub-assemblies, an emitter and a detector. Each of the two sub-assemblies contains an optical component as well as a photoelectric component. Figure 4 is a conceptual illustration of the unit. The unit projects the four different wavebands of light sequentially onto a designated target (i.e., only one waveband of light is emitted at a time). Light is reflected from the target and the unit detects reflected light at each waveband, sequentially.

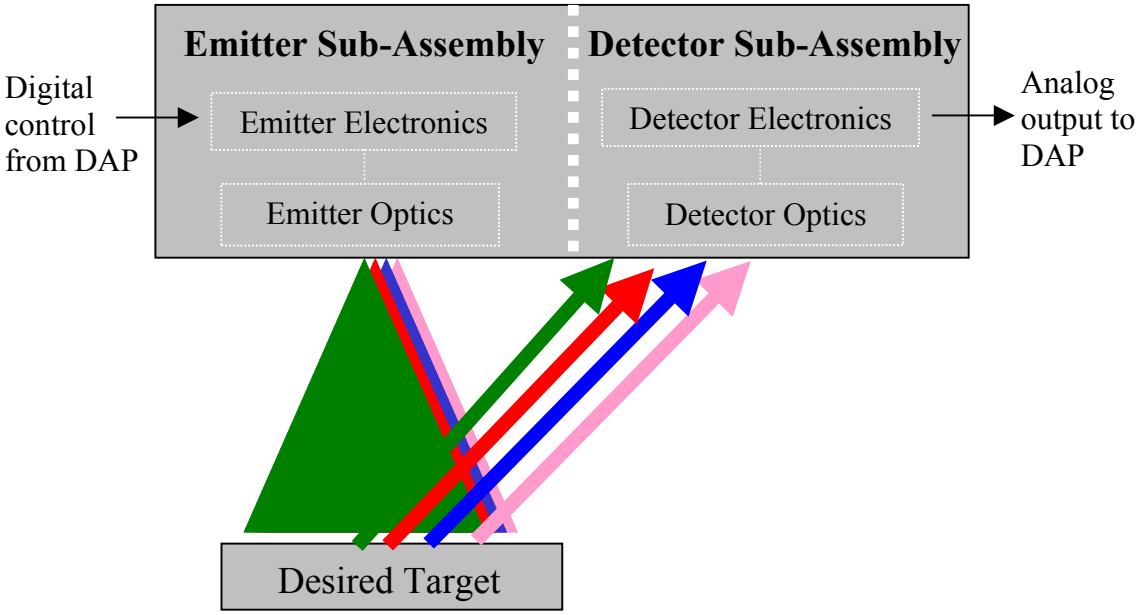


Figure 4. Concept of multi-spectral sensing unit.

Emitter Design

Overview

The first sub-system design goal was to design and fabricate an illumination source capable of emitting and projecting modulated multi-spectral bands onto a designated target. This goal led to an emitter design consisting of an electronic and optical system. The optical system consists of an array of LEDs and a focusing lens. The electronic system provides a modulated power drive circuit for the LEDs and digital control over waveband-specific LED selection. The following sections describe the design of the emitter's optical and electronic systems in detail.

Optical System

The light source must be modulated at a high frequency to allow filtering of the relatively low frequency response from ambient (sun) light. For this reason, LEDs were

used as the light source. Previous research has shown that wavebands of interest lie within the blue, green, red, and near infrared regions (Sui 1999). Wavelength range specifications were very important in the selection of individual LEDs. A number of LEDs within the required wavelength ranges (350-500 nm, 520-580 nm, 600-740 nm, and 750-1100 nm) were acquired and tested. Factors considered in diode selection included radiation intensity, pattern uniformity, and emission angle. Four ultra bright LEDs were selected within the desired wavebands for the final design (AND520HB, AND520HG, AND157HRP, and QEC123). Specifications for these LEDs are contained in Appendix B. All four of these LEDs emit approximately 20-degree cones of light with similar radiation intensity patterns. Rated luminous intensities are 1400, 5000, 1800, and 26,000 mcd and rated peak emission wavelengths are 466, 540, 644, and 880 nm for the blue, green, red, and infrared LEDs, respectively.

The desired projection target was a cotton plant canopy. Two requirements for light projection were established. First, the projection needed to span as much of the canopy width as possible without any significant percentage falling on soil between rows. Use of a large projection area would help to integrate spectral variations across the width of a plant canopy. Second, the highest light intensity possible should be projected onto the plant canopy for maximum sensitivity. These requirements contradicted one another. To reach an optimum balance, the LEDs were abutted to one another in a single linear array configuration. A plano convex (PCX) cylinder lens (C46-021, Edmund Ind. Optics) was used to collimate the cones of light emitted from the LEDs in one dimension (Figure 5.). This resulted in the projection of a high intensity scanning beam no wider than the minimum plant canopy (≅ 1 x 7 inches).

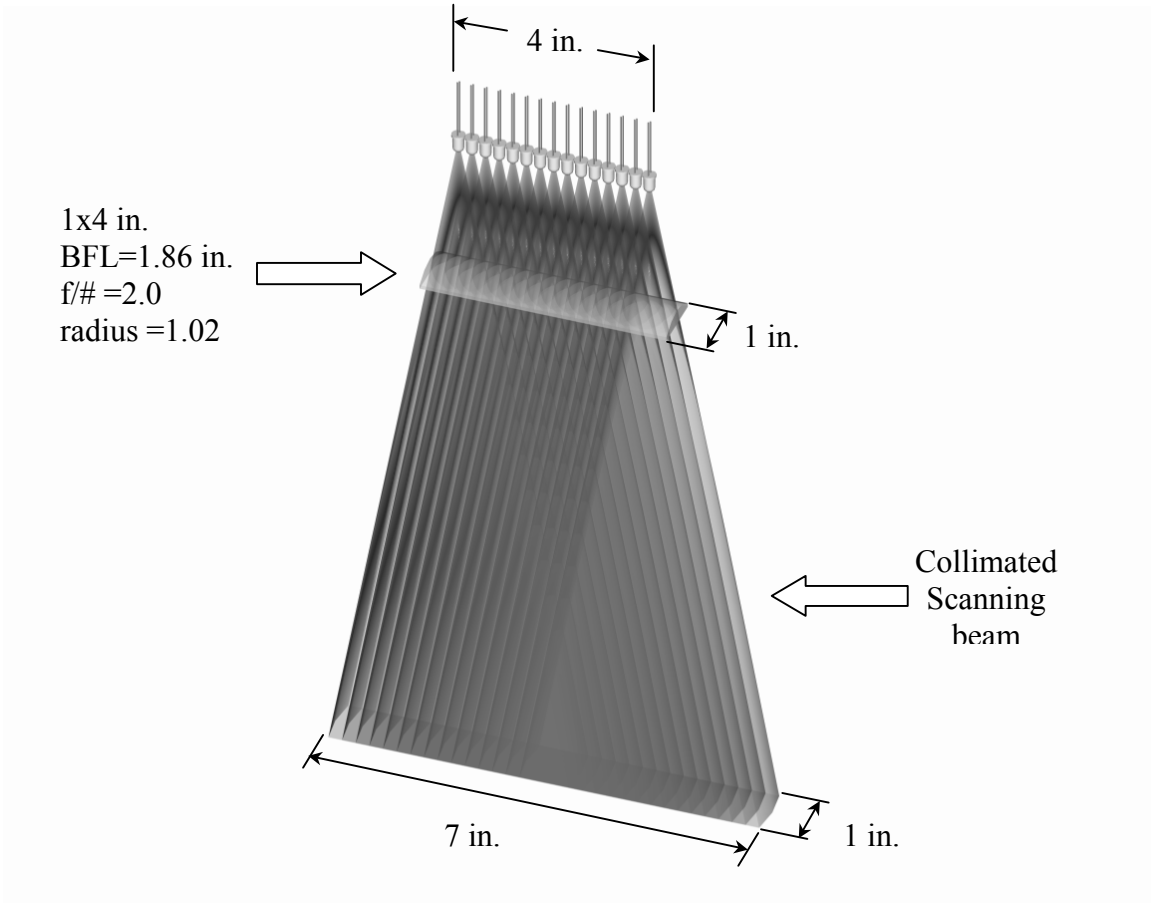


Figure 5. LEDs are aligned in a single array and light cones are collimated in one dimension to create a linear scanning beam.

Due to the reflectance characteristics of the plant canopy and the variation in radiation intensity, the number of waveband specific LEDs required in the prototype varied. To obtain a measurable quantity of reflectance in the blue and green wavebands, a larger quantity of these LEDs was required. LEDs were aligned in a single array with alternating colors throughout. Because of LED size, in this single array configuration, space limited the number of LEDs that could be used (15 unmodified). In addition to space

limitations, the single array configuration created some spatial offset in the light projection. To reduce the adverse effects of space limitations and spatial offset, material was removed from the LEDs with the two opposite sides each cut on a 0.5 degree angle (Figure 6). The removal of this material had very little effect on optical projection of light from individual LEDs. With the modifications made, nine more LEDs fit into the same space bringing the total to 24 LEDs (2 red, 2 infrared, 10 blue, 10green). The angle also eliminated most of the spatial offset by directing the center of each LED projection toward a single point ten inches away from the array (Figure 7). A clamping jig was used to ensure the alignment of the LEDs while they were soldered securely to the emitter electronic PCB. Stand-offs were used to secure the PCB to the lens holder. Figure 8 shows the fabricated prototype emitter assembly.

Electronic System

Figure 9 is a schematic of the emitter electronic circuit. An IC timer (555) is used to generate a square wave modulation signal at a frequency of 18.9 kHz with a duty cycle of 50%. Again, it is important to note that only one waveband of light is being emitted at a time. The modulation signal is connected to the enable pin of a 3-to-8 decoder (LS138) where the signal can be multiplexed to one of four different channels. A two-bit address controlled by the DAP system dictates which channel receives the modulation signal. Each channel is inverted using an inverter, leaving all channels low with the exception of the modulated channel. For discussion purposes, only signal flow through the active modulated channel will be considered from this point forward. The inverted modulation

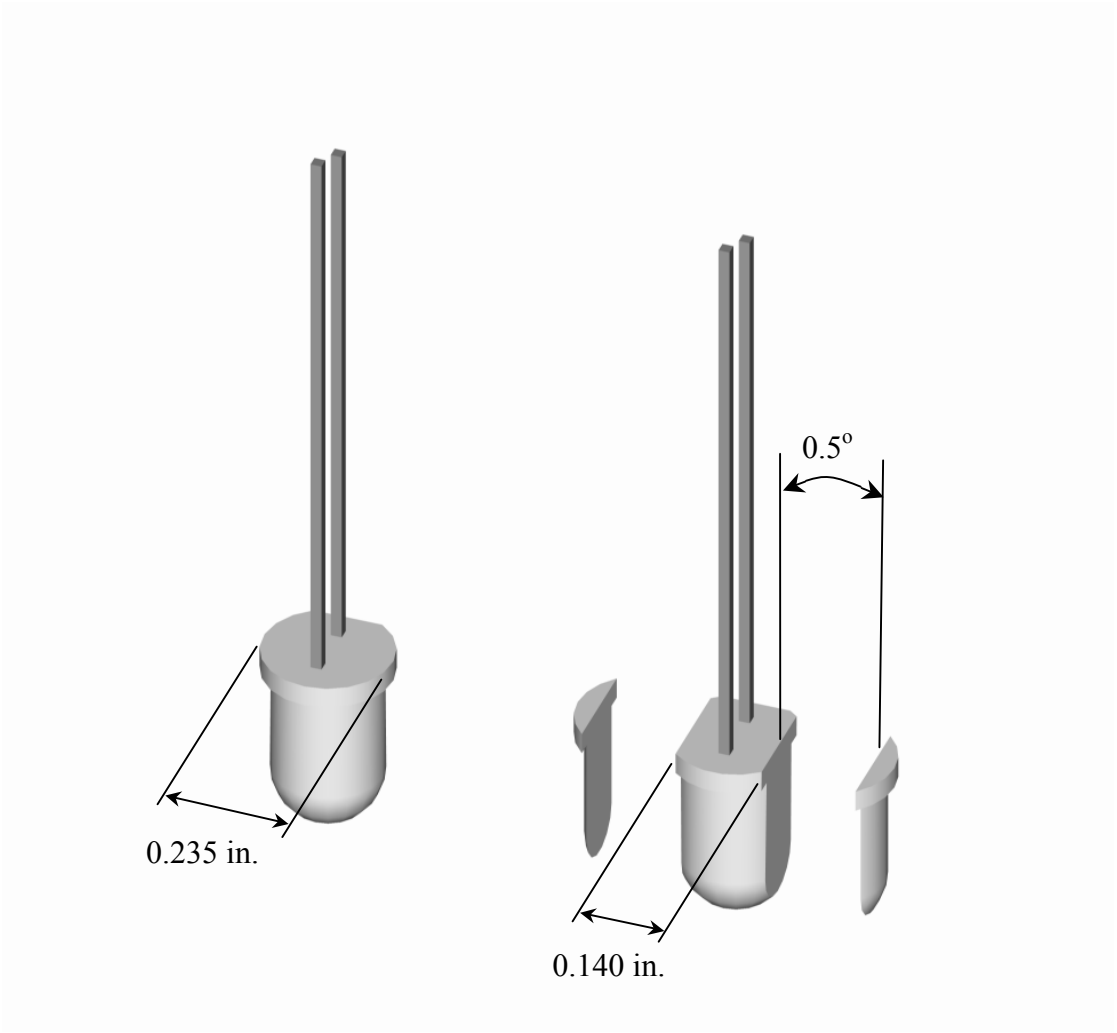


Figure 6. Portions of the LEDs were removed leaving an angle of 0.5 degrees on both sides of each modified LED.



Figure 7. Centerline of all LEDs are directed toward a single point ten inches from the LED array.

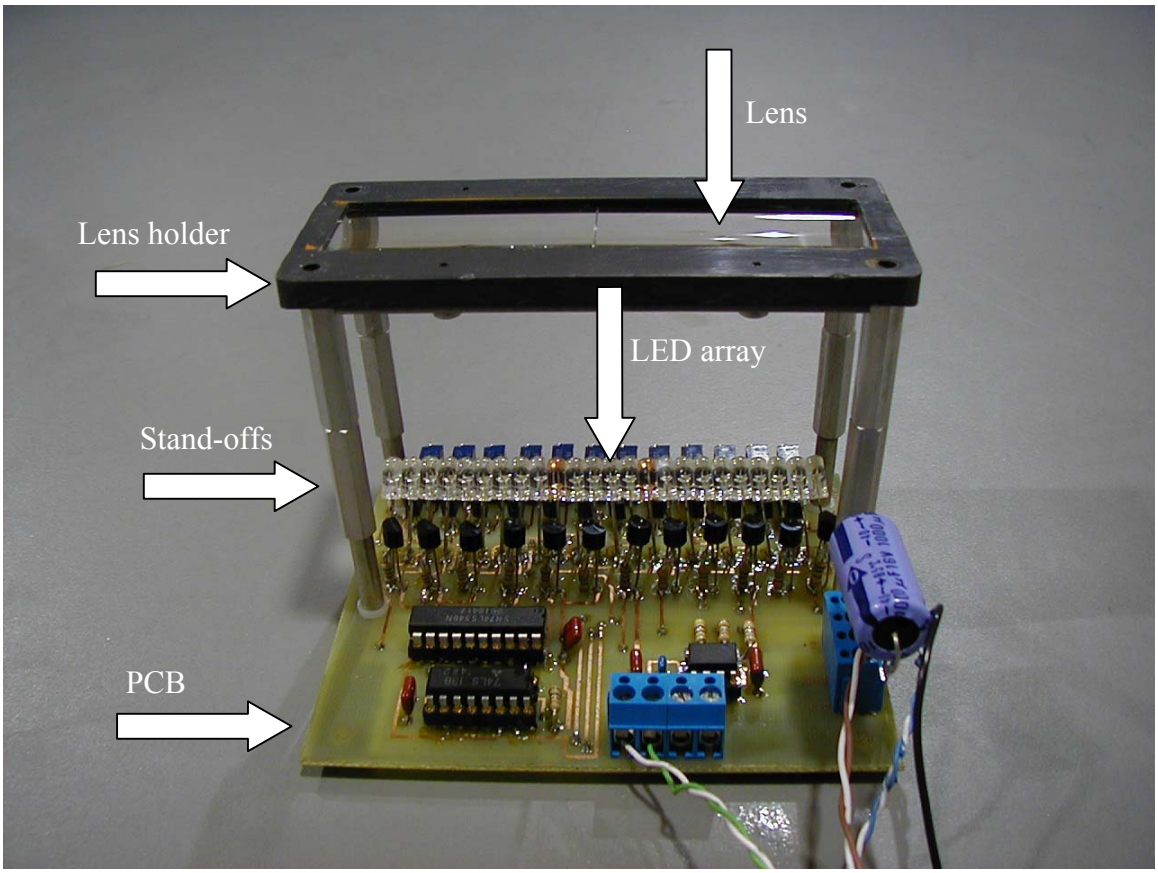


Figure 8. Fabricated prototype emitter assembly.

signal is connected to the base of one or more transistors, depending on the channel. The blue and green channels each have five transistors and the red and infrared each have one transistor. Two LEDs are connected in series to each of the 12 transistor collectors. A 12-volt potential drives the two LEDs in series with current limited by a current limiting IC (LM317). When the modulation signal is active high, the switching transistor saturates allowing current to flow through the LEDs (adjustable to 100mA). Thus, modulated light is generated at the driving frequency. Each channel operates in this same manner.

Emitter Sub-Assembly Mounting

The multi-spectral sensing unit housing is designed to provide alignment of the detector field-of-view with the emitter's light projection. The sensing unit is housed in a single enclosure with two sections. The divider wall optically isolates the emitter and detector sub-assemblies as shown in Figure 10. The two sub-assemblies are securely mounted in the enclosure for appropriate orientation.

The emitter sub-assembly is mounted in the housing unit by pressing the lens holder into a machined slot. Four machine screws secure the emitter sub-assembly to the housing. Figure 10 shows the emitter sub-assembly mounted inside the housing. Note that the LED array is parallel to the bottom of the housing. This ensures that the projection target center lies a perpendicular distance of eight inches away from the array.

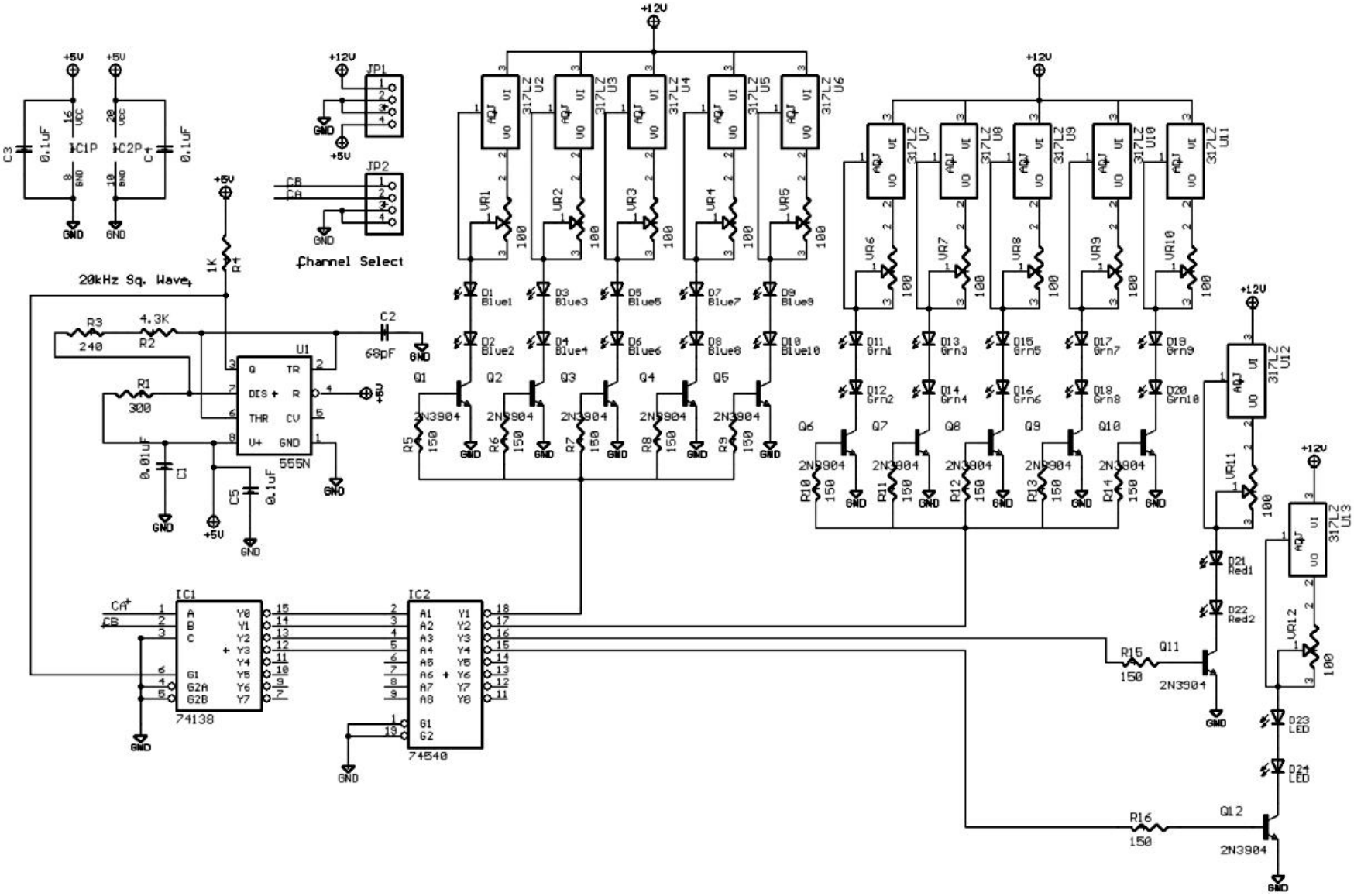


Figure 9. Emitter Board Circuit Schematic.

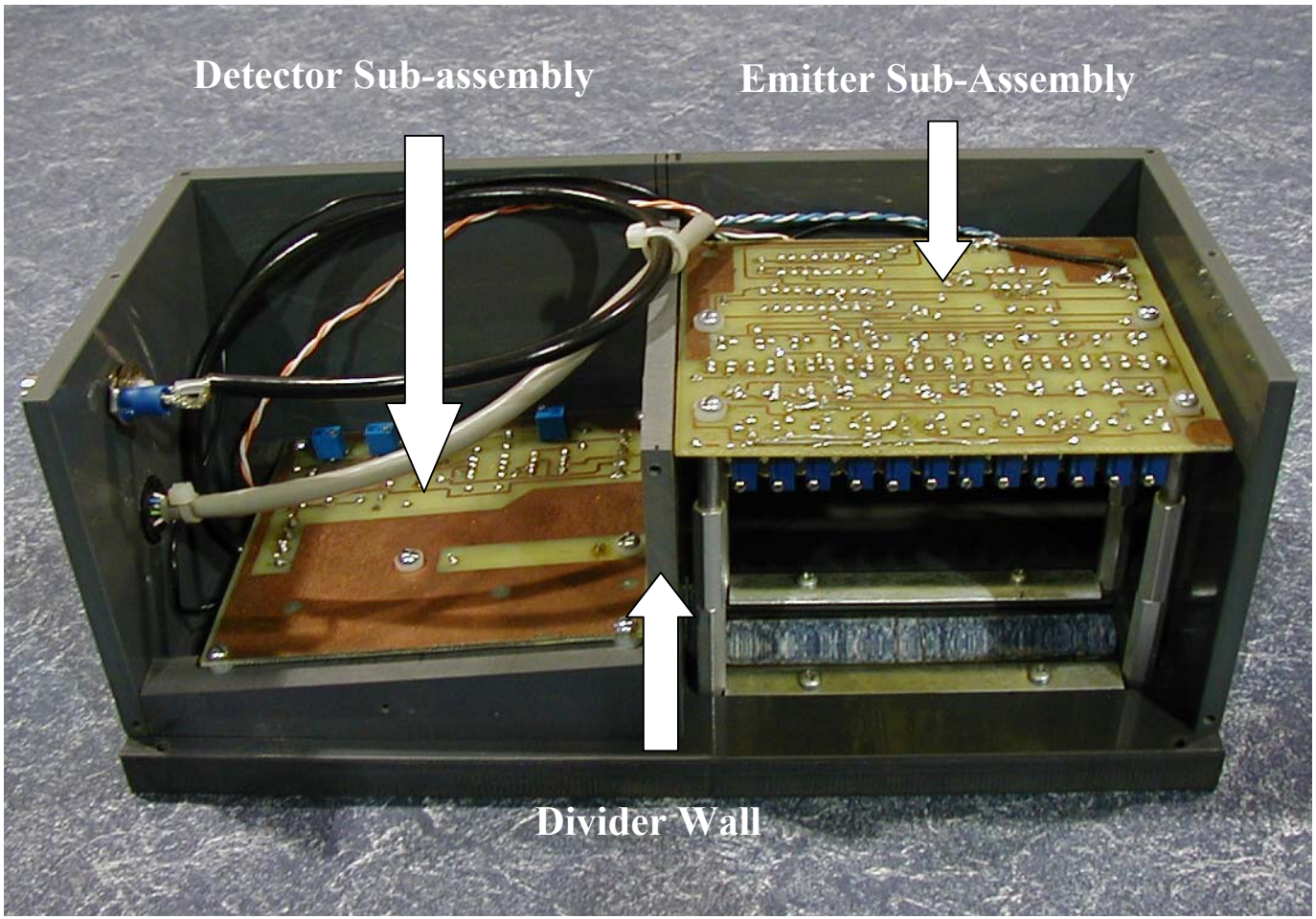


Figure 10. Sensing Unit with panel removed to reveal the detector and emitter sections.

Detector Design

Overview

The second sub-system design goal was to design and fabricate a sensor to detect only reflected modulated light intensity from the plant canopy. The detector contains an optical system and an optoelectric interface. The optical system focuses the reflected light onto a photodiode, and the signal processing circuitry converts only modulated light into a measurable voltage signal. The following sections describe the design of the detector's optical and optoelectric interface systems in detail.

Optical Sub-System

Optical components of the detector consist of a focusing lens and a photodiode. A double convex lens with a focal length of 2.835 inches and a diameter of 0.472 inch is used to focus reflected light from the target area onto a single rectangular photodiode. The field-of-view for the detector is only slightly larger than the emitter's projection. The field-of-view is constrained by the focal length of the lens and the geometric shape of the photodiode's active area. Only light striking objects inside the field-of-view will be directed onto the photodiode's active area. The photodiode is soldered to a PCB and the lens holder has been machined to fit directly over it (Figures 11 and 12). With the lens holder and photodiode securely mounted to the PCB, the detector field-of-view can be aligned with the emitted scanning beam.

A rectangular photodiode (0.0748 x 1.142 in), manufactured by Hamamatsu (part #2551), is used. Figure 13 illustrates photodiode relative response as a function of wavelength along with LED emission intensity. Note the relationship between LED emissions and photodiode response.

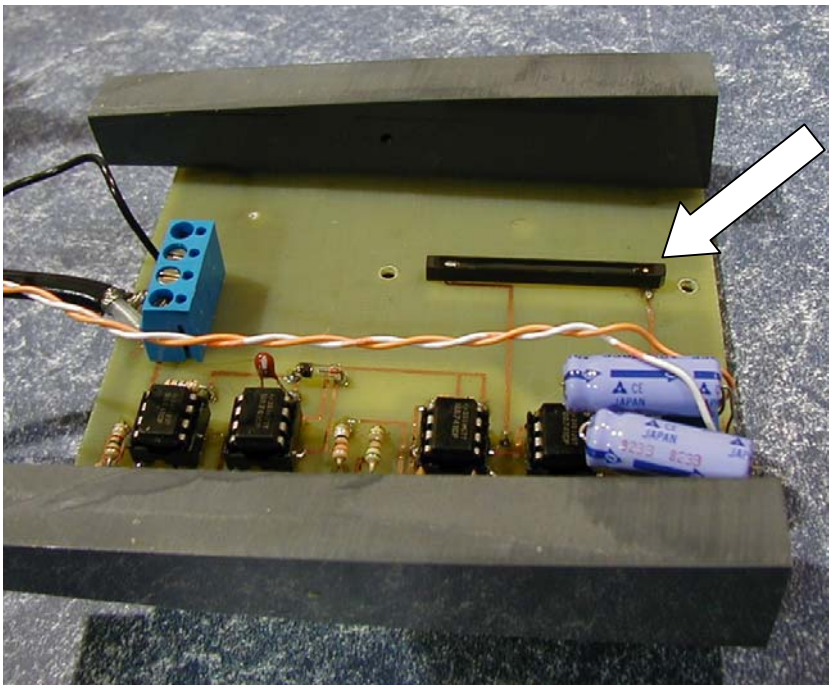


Figure 11. Photodiode soldered to PCB.

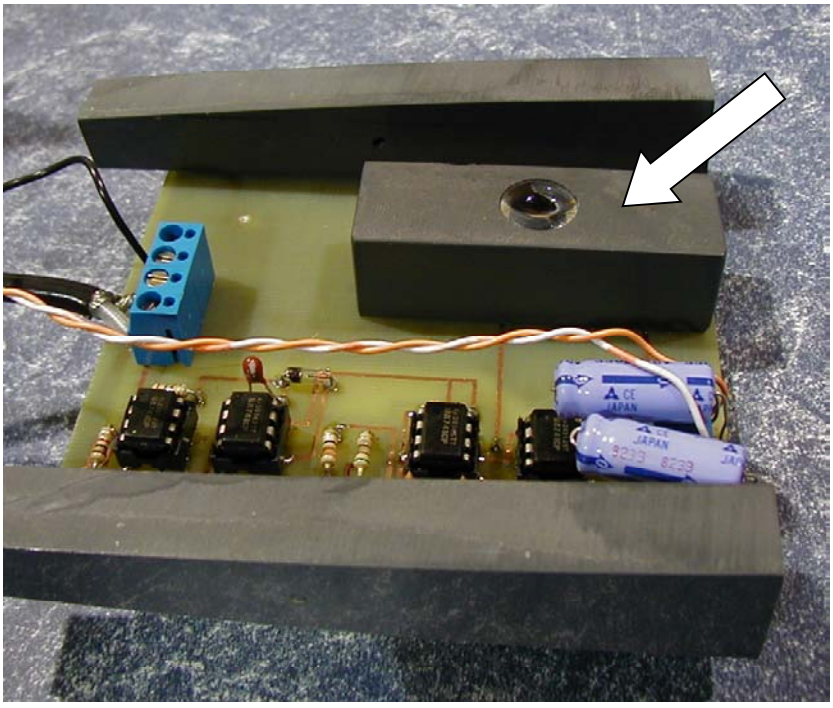


Figure 12. Lens holder mounted securely over the photodiode.

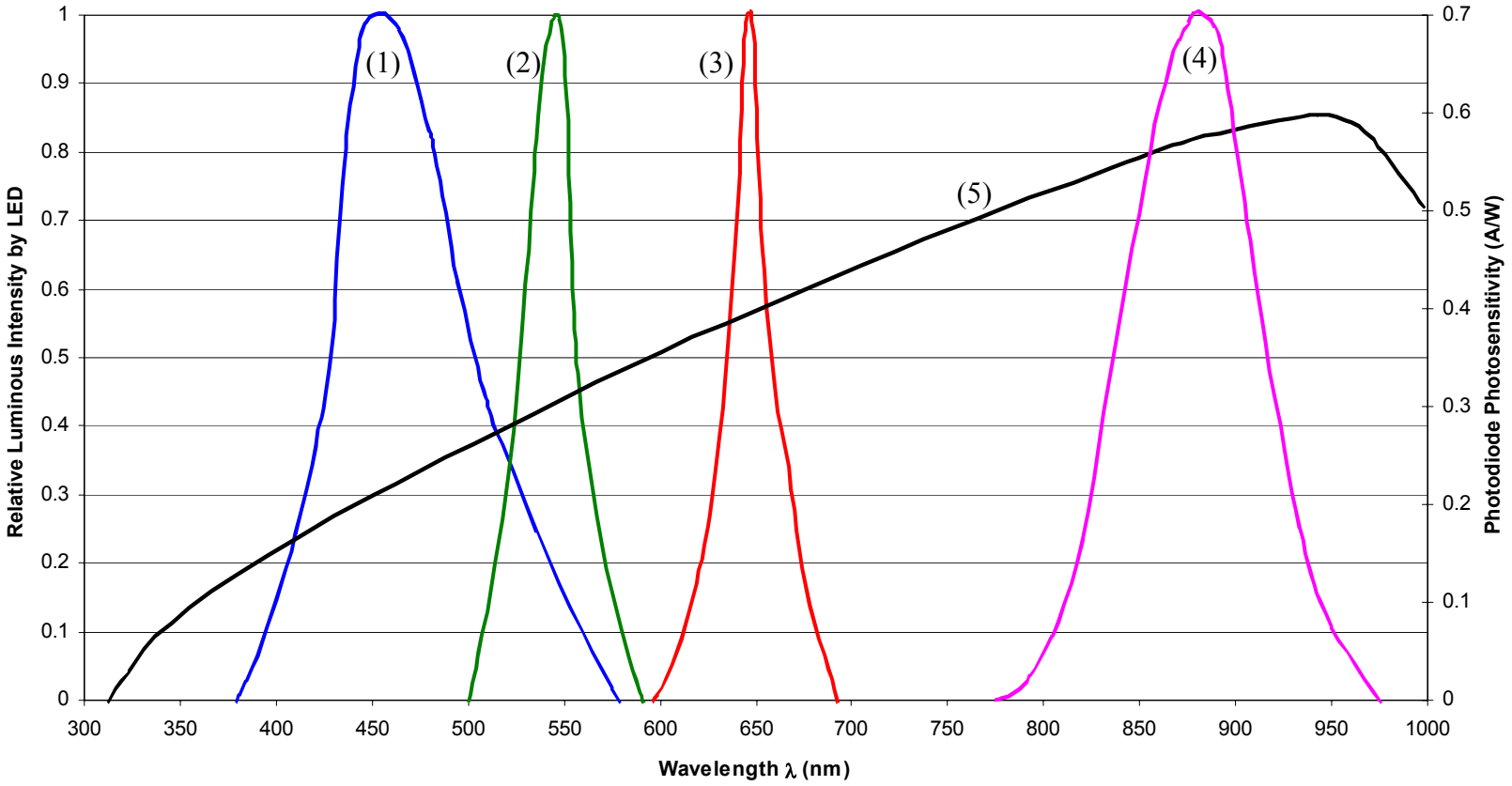


Figure 13. LED luminous intensities (1-blue, 2-green, 3-red, 4-NIR) and photodiode response (5).

Optoelectric Interface

Figure 14 is a schematic of the detector signal processing circuit. Modulated light and low frequency ambient (sun) light are reflected by the plant canopy and focused on the photodiode. The photodiode is excited and produces AC current proportional to the reflected energy from the modulated light and DC current proportional to the reflected solar energy. A simple current-to-voltage circuit is used to produce a voltage signal representing both AC and DC components. Sunlight contains a full spectrum of light energy, and only the wavelength ranges emitted by the LEDs are of interest. Therefore, the DC signal component (the sunlight) is filtered out using an active analog band-pass filter. Cutoff frequencies of 17 kHz and 22 kHz allow the modulation frequency to pass while attenuating frequencies outside this narrow band. Figure 15 shows the frequency response of the active band-pass filter. An amplification circuit follows the band-pass filter. Following the amplification circuit the signal is demodulated using a diode and an R-C network. The demodulated signal is amplified a final time to obtain a signal within a 0 to 10 volt range. This analog DC signal is connected to a coaxial connector (BNC) mounted in the housing of the sensing unit. The analog signal is transmitted to the DAP box via coax cable.

Detector Sub-Assembly Mounting

The detector sub-assembly is mounted in the housing unit at an angle of 10 degrees to align its field-of-view with the emitter's light projection. A wedge block is mounted to each side of the detector PCB. The wedges are cut on a 10-degree angle. Secured to the PCB, the wedges are mounted inside the housing. Figure 16 shows the detector sub-assembly mounted in the housing and illustrates how the optics are aligned.

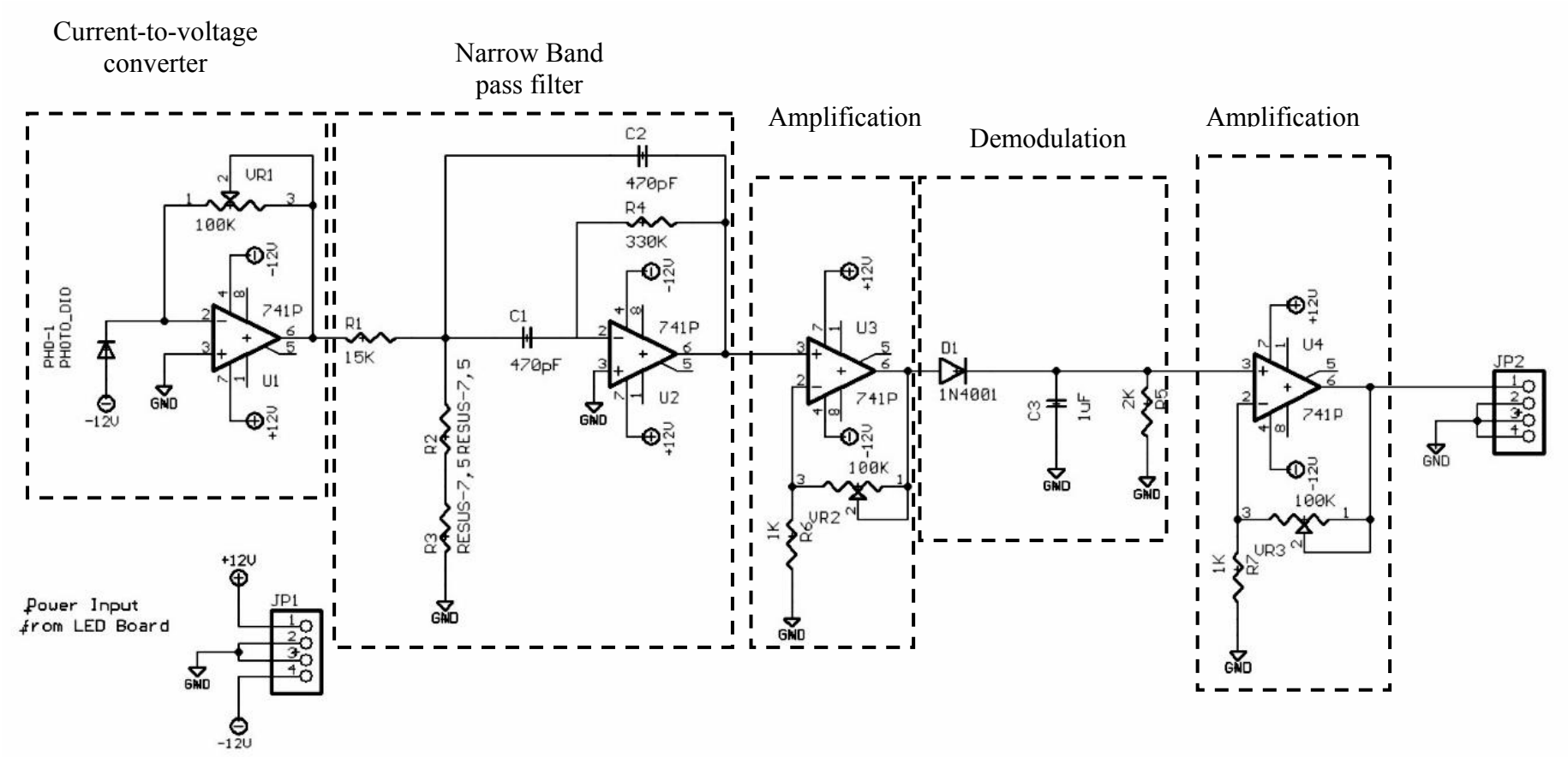


Figure 14. Optoelectric interface Board Circuit Schematic.

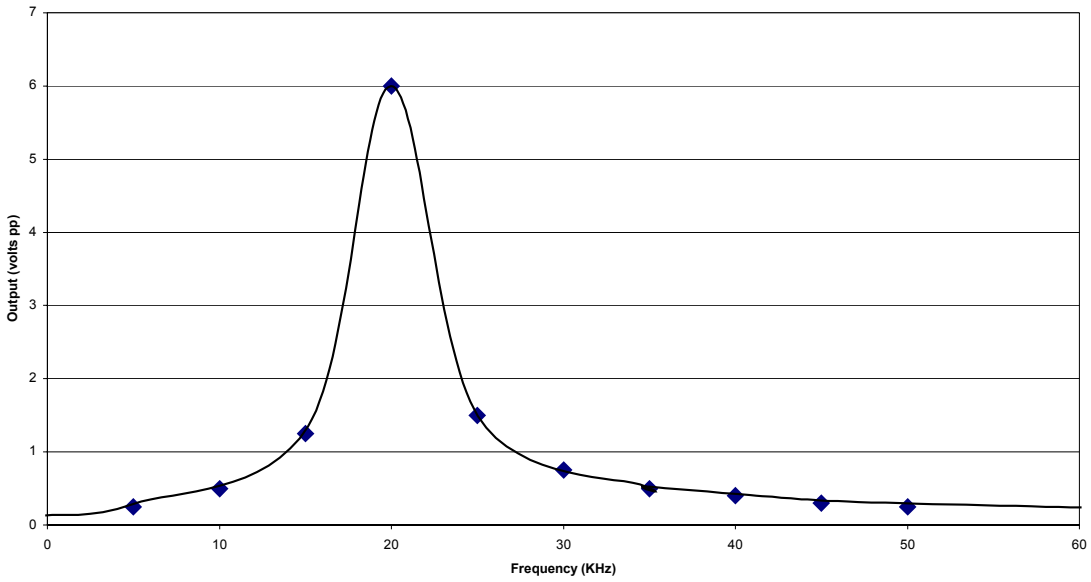


Figure 15. Measured band pass filter (with gain) response to a one-volt sine wave.

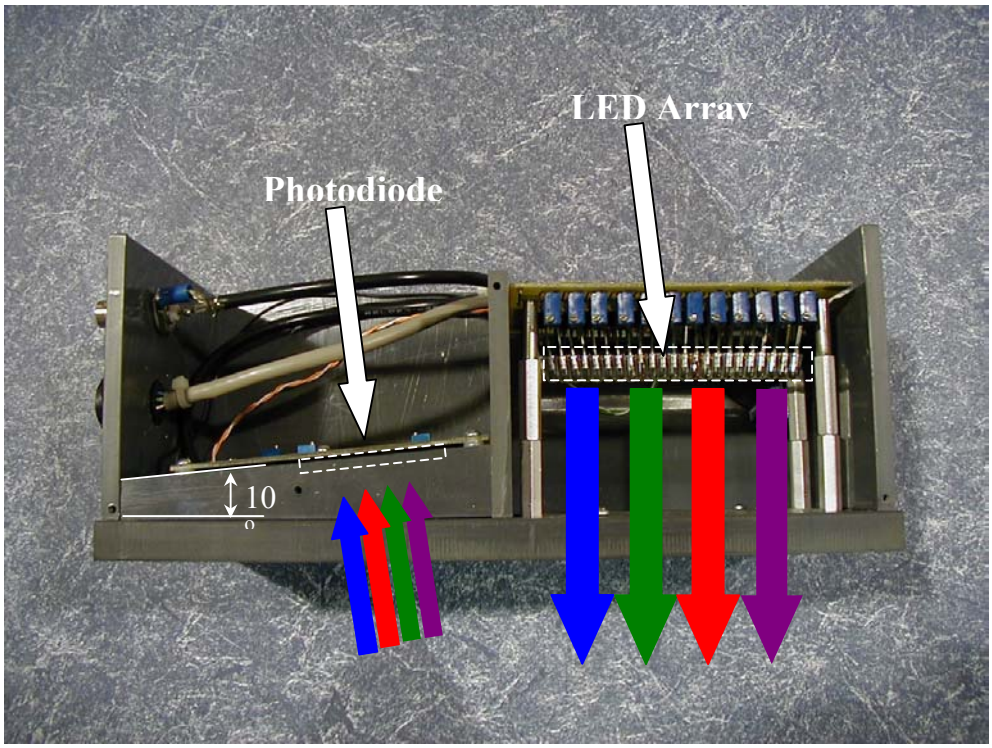


Figure 16. Photodiode and LED array orientation.

Data Acquisition and Processing System Design

Hardware

Overview

A reliable data acquisition and processing system was needed to operate in a roughed field environmental with elevated temperatures, high moisture, vibrations, and dirt. The data acquisition and processing system consists of an industrial single board computer, interfaced via a PC104 bus with an Analog to Digital converter (ADC) and a PCMCIA card drive (figure 17). The PCMCIA card drive and ADC are mounted to the single board computer in a PC104 stack configuration. A PVC box was built to house this assembly along with a power regulation circuit. Power requirements for the DAPS and the multi-spectral sensing unit are fulfilled by this power regulation circuit. Power and digital control is supplied to the sensing unit through a wiring harness. The DAP system receives analog spectral reflectance signals via coax cable.

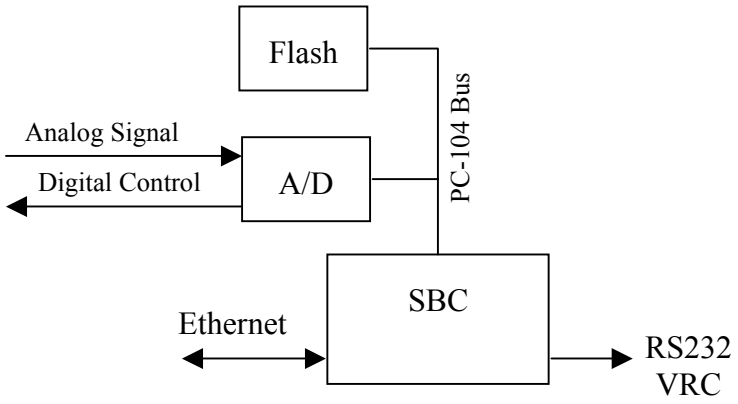


Figure 17. Data Acquistion and Processing schematic.

Single-board Computer

A PC-680 manufactured by Octagon Systems Corporation was used in the design of the system. Specifications for the PC-680 are included in Appendix B. The computer utilizes a Pentium Processor with a clock speed of 133 MHz. A 72 MB Disk-on-Chip solid-state drive from M-Systems was added for reliable storage of the operating system. A PC-104 interface allowed for the addition of a PCMCIA card drive (SDDP-21, Adtron Corporation) and a 12-bit A/D (PC104-DAS08, Measurement Computing, Corp.). PCMCIA flash disks are used for storage devices. The A/D has 7-bits of digital I/O and eight analog input channels with a maximum sample rate of 20 KHz. Two bits of digital output are used to control LED modulation in the multi-spectral sensing unit. One analog input channel is used to convert the output of the sensing unit to a digital reading.

Graphical User Interface

A Compaq iPAQ H3635 Pocket PC serves as a graphical user interface for the system. The iPAQ is interfaced with the PC 680 via a compact ethernet card and T-Base 10 cable. Networking is performed using TCP/IP protocol. Using Virtual Networking Communication Software by AT&T the iPAQ was used as a dumb terminal for the DAP system. This software enabled the DAP system's video output to be captured and viewed on the IPAQ screen. A 2.26 by 3.02 inch color reflective TFT liquid crystal display along with a touch screen provided excellent control of the system. The iPAQ was chosen because it provides excellent viewability, even it bright sunlight.

Power Requirements

The DAP system requires three voltage supplies for operation: ±12, and +5 volts. Five volts is required for the single board computer, and ±12V for the A/D and analog processing circuits contained in the sensing unit. For a typical agricultural application,

vehicle supply voltage is 12 volts. A triple output DC-to-DC converter (part #PM3012TO512, Lambda) is used to convert the availability 12 volt supply to the required voltages. The DC-to-DC can operate with an input range of 9-18 volts. A self-contained rechargeable battery powers the Compaq iPAQ.

Software for Data Acquisition and Processing

The operating system running on the single board computer is Microsoft Windows 95. Footprint of the operating system was minimized to fit on the Solid State Disk-on-Chip. Visual Basic 6.0 was used to create the software for system control and data acquisition. For ease of operation, an executable was created from a Visual Basic module that provided large display buttons on the IPAQ's screen. Matlab with the Neural Network Toolbox was used to train and test a neural network.

Data Acquisition Program

A Visual Basic program was implemented to control the process of spectral data acquisition. A flow diagram of the program is shown in figure 18. When the program executes, the first wavelength specific set of LEDs modulate. A pause of 0.05 msec is executed to allow the signal processing circuit to stabilize. After the pause, a voltage reading is acquired corresponding to the light reflected for that wavelength. Immediately afterwards the next set of LEDs are modulated and the process is repeated until all four measurements have been obtained and the results written to a file. This is considered a single scan, and executes in approximately 2.5 msec. The program checks for a stop command from user input after each scan.

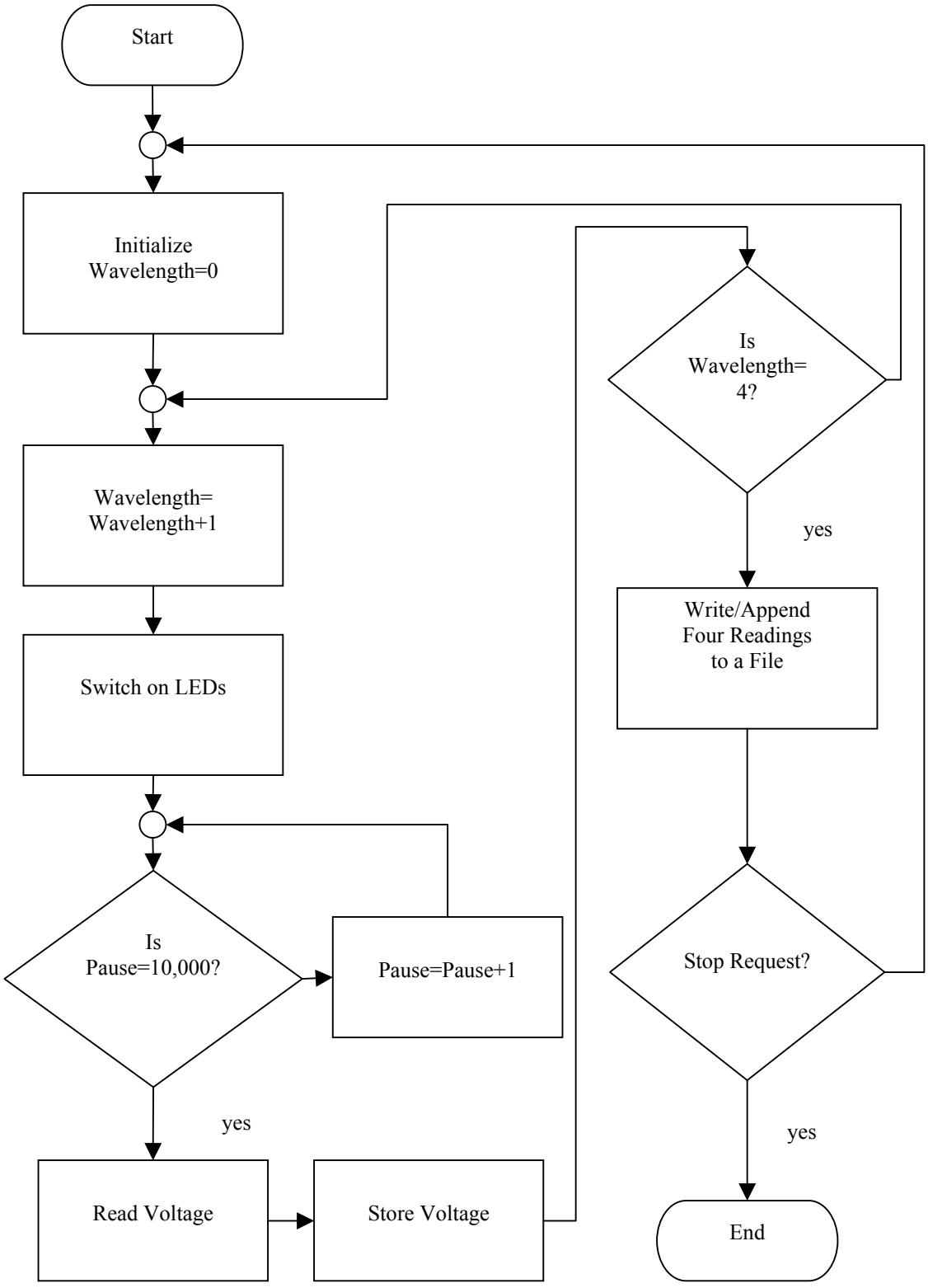


Figure 18. Flow diagram of Visual Basic Data Acquisition Program.

Neural Network

A backpropagation algorithm was used in supervised training of a multilayer feedforward neural network. Network training was implemented using Matlab with the Neural Network Toolbox. Using four different reflected light measurements as inputs, a network was trained to predict N status with a linear output. Matlab code for the training program can be found in Appendix C. Weights and biases were randomly initialized. Backpropagated through the network, error is minimized by adjusting the weights and biases. This learning process was repeated until an error goal or the maximum number of training epochs was reached. The network was saved for evaluation using testing data sets.

Also implemented using Matlab with the Neural Network Toolbox, the trained neural network was used to generalize nitrogen status. Matlab code for the testing program can also be found in Appendix C. Weights and biases, saved from the training process, were implemented in the testing of the trained neural network. Prediction of nitrogen status accuracy was calculated for each the test data sets.

Testing Procedures

Experimental Plot Layout

Experimental plots were established at The University of Tennessee Jackson Agricultural Experiment Station in 2001. Cotton (DP451 BRR) was planted with a row spacing of 40 inches. Plots were established to create varying levels of nitrogen stress in conventional tillage conditions. Application rates of 0, 30, 60, and 90 lbs per acre of ammonia nitrate fertilizer were randomly applied to each plot. Four replications of each

application rate were used in the study giving a total of 16 plots. One row in each plot was used for this study. Each 20-foot row was split giving a total of 32 experimental units.

Spectral Data Acquisition

Using the prototyped system, reflected light measurements were randomly taken over a two day period in varying atmospheric conditions. To evaluate the system in worst case conditions, a significant percentage of the data was taken with no cloud cover and the highest solar angle. At the time of data acquisition, cotton plants were at a growth stage of pinhead square. Plant canopy heights ranged from 17 to 38 inches. Canopy height tended to increase significantly with nitrogen application rate. One condition affecting reflected light intensity of concern was wind rolling over plant leaves. Pausing data collection until conditions improved minimized this phenomenon.

The sensing unit was held by hand approximately 4 to 6 inches above the plant canopy. Dynamic and static runs were performed on each experimental unit. Dynamic runs were performed by continuous data collection from one end of the experimental unit (1/2 of 20 foot row) to the other at approximately one mile per hour. During the dynamic runs, the sensing unit was adjusted vertically to account for variations in plant canopy height. Static runs were performed by individually collecting 10 seconds of data on multiple plants within a plot. Each static run consisted of appended data from 5 to 6 plants. A total of 64 files were collected and collectively make up two data sets (dynamic and static).

Ground Truthing of Experimental Data

Plant Nitrogen Measurements

The uppermost fully developed plant petiole was collected from 10-12 randomly selected plants in each plot. Petiole samples from each plot were analyzed for N as a composite. A total of 32 composites were collected and analyzed for nitrate content. In parallel with composite sample collection, spectral scans were collected with the prototyped sensing system.

Nitrate content of petiole sample were analyzed using a laboratory procedure established by the soil-testing laboratory at the University of Arkansas (1991). Petiole samples were dried at 83 ^{o}C for 48 hours in a forced air drying chamber. Petiole samples were then ground to pass a 20-mesh screen. An extraction solution of aluminum sulfate and deionized water was prepared at 12 g/L. To eliminate interferences in nitrate measurement, nitrate ionic strength adjustor was added to the extraction solution. The strength adjustor consisted of 0.264 g of 2M$(NH_4)_2SO_4$ per 1 mL of deionized water. Approximately 0.08 to 0.15 grams of each ground composite were placed in individual flasks with 100 mL of extraction solution. For proper extraction, flasks were shaken for one hour. After shaking, nitrate content was measured using a nitrate electrode (ORION, 1990) with a Model 290A pH meter (ORION, 1991).

Plant Nitrate Analysis

Petiole nitrate analysis was used to validate the existence of plant N stress. Figure 19 shows the relationship between the measured petiole nitrate (ppm) and soil applied nitrogen application rate (lbs/acre). Each point represents a composite nitrate measurement for each experimental unit. Measured petiole nitrate had a moderate correlation with N application rate (r^2=0.7492) based on data from one season. Note that no significant

increase in plant nitrate is observed in the higher application rates. This relationship is very similar to that reported by Sui (1999). Between 60 and 90 lbs per acre, no statistical difference in petiole nitrate content was found (α=0.05). Based on this observation, N application rates higher than 60 lbs per acre do not significantly increase plant N uptake. Cotton plants with high N stress have been determined to have a petiole nitrate content of less than 25,000 ppm (Benton et al., 1979). In this study, the range of nitrogen levels in the plants used for sensor testing did not adequately represent the low range for plant N (i.e. <25,000 ppm). However, the nitrate analysis did validate the existence of moderate N stress variation within the experimental plots. Based on this analysis, N status was defined by three classes: low(0 lbs/acre), medium(30 lbs/acre), and high(60 and 90 lbs/acre). Corresponding to three N status classes, discrete N status values are used as the dependent variable in arbitrary units (0, 30, and 60).

Neural Network Training and Testing

A feed-forward neural network was trained and tested to predict nitrogen status using spectral data taken with the prototype sensing unit. Four inputs presented to the neural network were cotton canopy reflected energy measurements (blue, green, red, and infrared) taken with the prototype system. A single linear output representing nitrogen status was utilized. With the input and output layers defined, size and number of hidden layers was determined based on the networks ability to appropriately fit the available data. Larger network architectures will tend to overfit the training data set and be unable to generalize well. Networks that are too small will be unable to learn the desired function. Different architectures were evaluated to determine the optimum network. The network

was trained and tested with desired discrete outputs of 0, 30, and 60. To prevent biased networks, training and testing data contained equal distribution of each discrete output with corresponding inputs. Table 1 shows percentage of data used for training and testing with different collection and extraction methods. Training and testing was performed for eight different scenarios. Systematic data extraction refers to systematic selection of scans without replacement from the dynamic and static data sets. Consecutive data extraction refers to sequential selection of data from the dynamic and static data sets. A spectral index and linear regression were evaluated in parallel with the neural network for comparison using the same data and extraction methods.

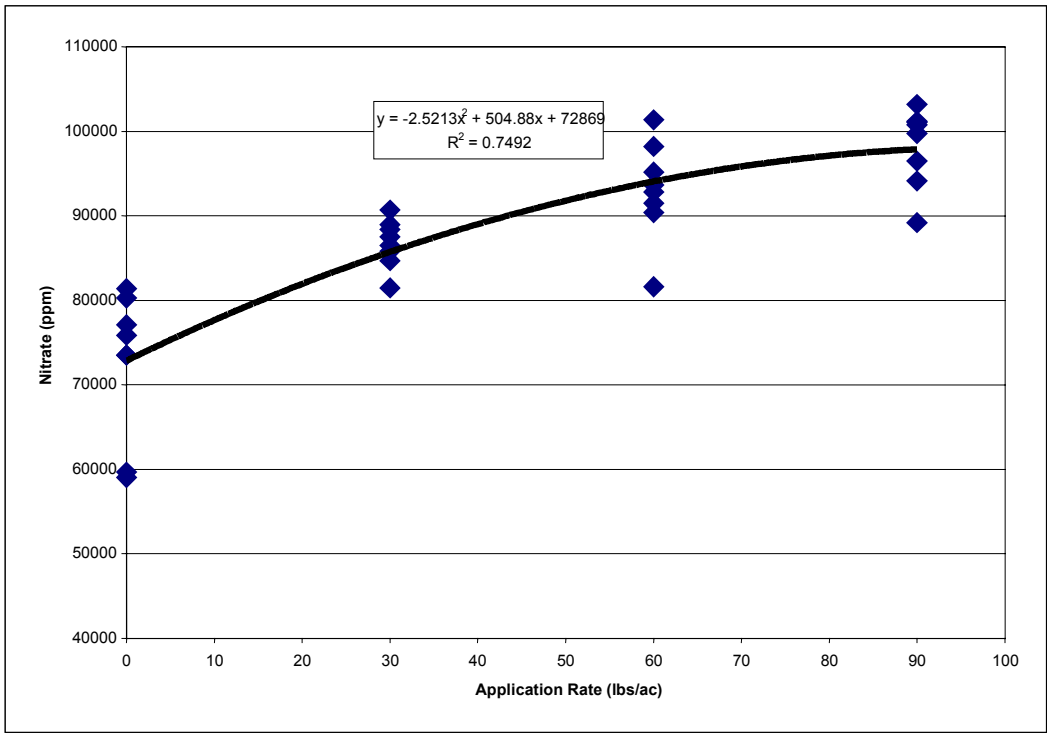


Figure 19. Nitrate measurements in ppm as a function of nitrogen application rate.

Table 1. Data percentages used for training and testing.

Scenario	Data extraction	Collection Method	% data for training	% data for testing
1	Systematic	Dynamic	50%	50%
2	Systematic	Dynamic	25%	75%
3	Systematic	Static	50%	50%
4	Systematic	Static	25%	75%
5	Consecutive	Dynamic	50%	50%
6	Consecutive	Dynamic	25%	75%
7	Consecutive	Static	50%	50%
8	Consecutive	Static	25%	75%

Data Post-Processing

Based on a preliminary analysis of data, no significant correlations were found between N status and spectral measurements. During data collection, modulated light was projected partially onto soil in sparse canopies. This observation was a major concern. To eliminate reflected light from soil, spectral data was filtered. As shown in figure 20, soil scans are distinctive with the ratio of red to infrared proving to be a good indicator of soil. Through preliminary analysis of several well documented combined soil and plant dynamic scans, a soil indicator was determined from a ratio of red to infrared. Using a soil indication ratio of 0.7, soil was removed from spectral scans.

Through further preliminary analysis, sensitivity to unrepresentative spectral characteristics in the field-of-view was defined as a problem. This problem appeared in the form of voltage spikes due to high reflectance. These spikes could be due to leaf roll over or the sensor was too close to the canopy. An amplitude threshold of 4.5 volts was used to filter out each scan that contained a spike in any one of the four spectral bands. Average

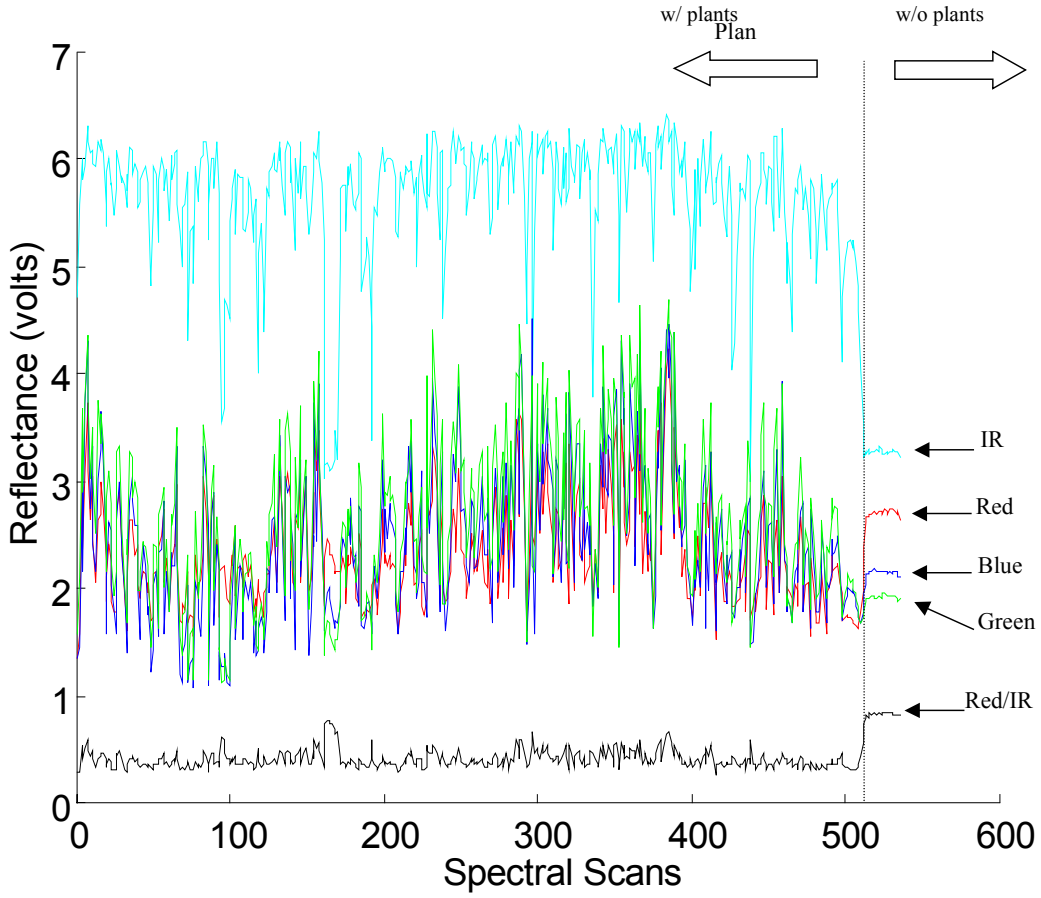


Figure 20. Example of soil at end of crop row.

infrared emission intensity was reduced for final data collection, therefore figure 20 is not representative of data which is to be filtered. Reported results are determined from data unless specified otherwise.

CHAPTER IV. RESULTS

Spectral Band Correlations with N Status

Correlations between spectral data and N status were analyzed. Using raw data, no significant correlation (α=0.05) was found between any one waveband and N classification. However, spectral data filtered based on signal strength and a soil indication ratio improved the correlation. As described in the testing procedures section, dynamic data was collected continuously from one end of the experimental unit (1/2 of 20' row) to the other and static data was collected by combining five to six individual plant scans. Table 2 provides correlation coefficients created from data acquired dynamically and table 3 provides correlation coefficients created from data acquired statically. With correlation coefficients of –0.7285 and -0.6123, reflectance in the red region has the highest correlation with N status. A negative correlation in this region is consistent with increasing "greenness" of plant canopy. "Greenness" due to chlorophyll content has been shown to increase with N uptake (Wood et al., 1992). As chlorophyll content increases, reflectance intensity in the red region (chlorophyll absorbing) is expected to decrease. Linear correlation results indicate little information can be derived from any one of the other three waveband measurements.

Table 2. Correlation coefficients matrix created from dynamically acquired data.

	BLUE	RED	GREEN	INFRARED	N Status
BLUE	1.0000	0.5025	0.8241	0.2738	-0.0984
RED	0.5025	1.0000	0.5928	0.0700	-0.7285
GREEN	0.8241	0.5928	1.0000	0.4228	-0.1391
INFRARED	0.2738	0.0700	0.4228	1.0000	0.2647
N Status	-0.0984	-0.7285	-0.1391	0.2647	1.0000

Table 3. Correlation coefficients matrix created from statically acquired data.

	BLUE	RED	GREEN	INFRARED	N Status
BLUE	1.0000	0.2838	0.8074	0.1475	0.0980
RED	0.2838	1.0000	0.3592	0.1943	-0.6123
GREEN	0.8074	0.3592	1.0000	0.3259	-0.0579
INFRARED	0.1475	0.1943	0.3259	1.0000	0.1003
N Status	0.0980	-0.6123	0.0579	-0.1003	1.000

Neural Network

A multiple layer perceptron was trained and tested to predict nitrogen status using spectral data taken with the prototype sensing unit. Different architectures were evaluated for prediction accuracy. Figure 21 graphically illustrates the optimum network architecture used for predicting nitrogen application rate. Input and output layers were defined by the function that the network is attempting to approximate. As described in the testing procedures section, the network is given four inputs (blue, green, red, and infrared) corresponding to reflected light intensity at four different wavebands. The network has a single linear output representing N status. Desired output ranges from 0 to 60. A sigmoid hidden layer was used to allow the network to learn possible non-linear relationships between spectral measurements and N status.

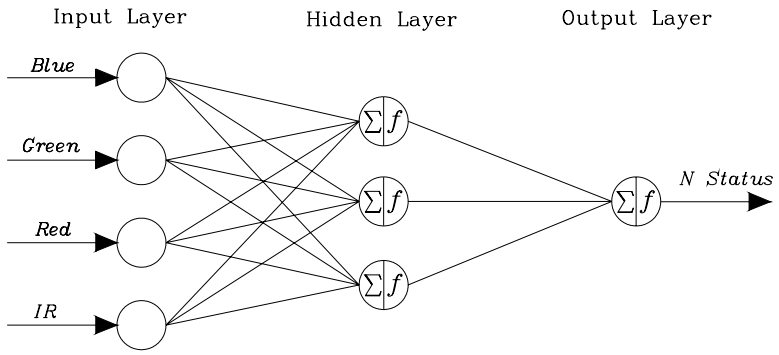


Figure 21. Optimum network architecture for diagnosing nitrogen status.

Classification thresholds were established for testing the network since desired outputs are discrete and network output is continuous. During testing, network outputs were grouped into three categories: low, medium, and high N. Thresholds were used to obtain the three N classifications. Evenly splitting the desired discrete output values, thresholds were set at 15 and 45. Figure 22 illustrates the placement of thresholds to achieve three classifications. Table 4 lists the results of neural network prediction with a decision made after each individual scan (i.e. no data smoothing). Equal number of input scans for each N classification was used during training and testing. Classification accuracy was calculated using the same thresholds for all testing.

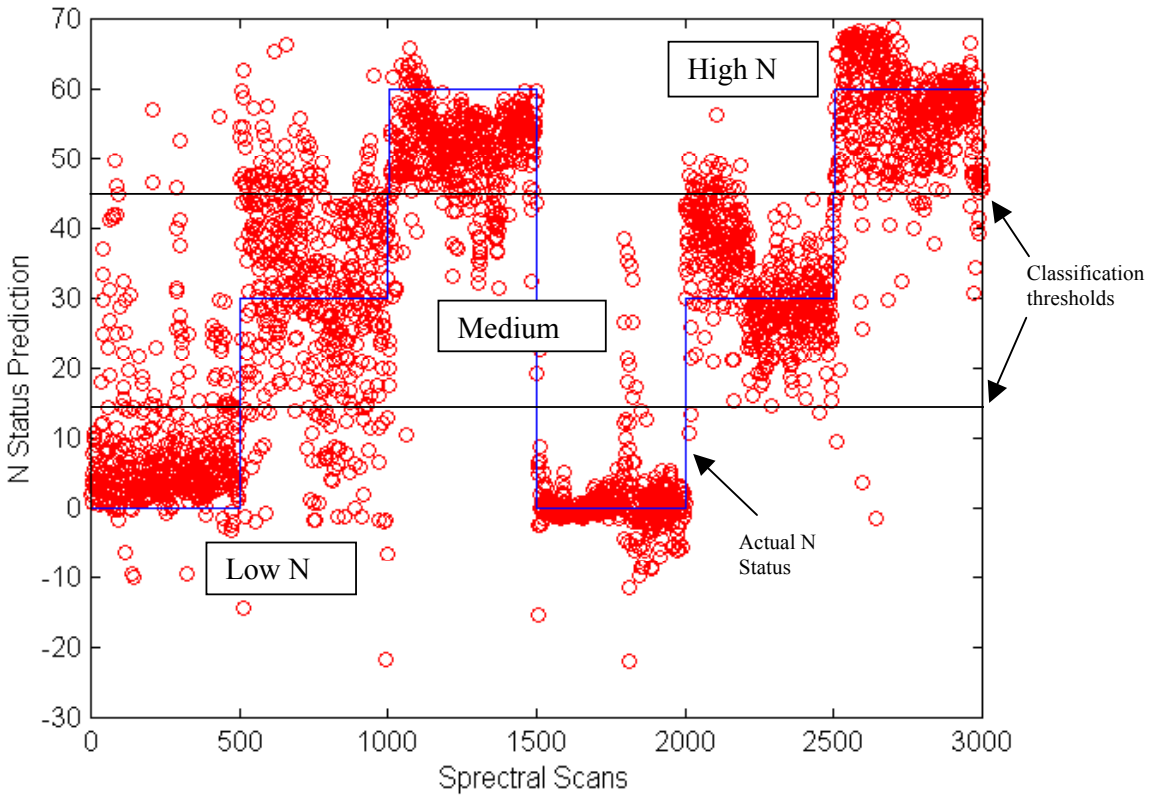


Figure 22. Three classification categories for N status.

Classification accuracy was higher using the dynamic collection method. This could be explained by the collection of more representative scans during the dynamic acquisition of data. As stated in the procedures section, the static collection method only represents five to six plants from each experimental unit. Each experimental unit contained 10 to 15 plants (≈1 plant/ft.). While collecting data using the static method, the potential exists to collect data from one unrepresentative plant resulting in a biased observation for that plot. Dynamic data collection provided a more representative sample from plants in each experimental unit.

Decisions made every scan are neither practical nor feasible, since any given scan potentially contains reflected light energy from soil or unrepresentative plants. Therefore, it was determined that decisions should be made based on a majority rule based on several single scan decisions. As scans per decision increased prediction accuracy increased for most test scenarios. Maximum accuracy was achieved at ten scans per decision, which resulted in scans covering approximately one foot or one plant canopy. Table 5 shows the improved accuracies at ten scans per decision.

Table 4. Summary of results with decision made every scan.

Scenario	Data extraction	Collection Method	% data for training and regression	% data for testing	Neural Network Accuracy	Regression Model Accuracy	NDVI Model Accuracy
1	Systematic	Dynamic	50%	50%	87%	75%	60%
2	Systematic	Dynamic	25%	75%	86%	74%	58%
3	Systematic	Static	50%	50%	76%	65%	42%
4	Systematic	Static	25%	75%	72%	63%	41%
5	Consecutive	Dynamic	50%	50%	66%	54%	43%
6	Consecutive	Dynamic	25%	75%	76%	67%	53%
7	Consecutive	Static	50%	50%	51%	44%	37%
8	Consecutive	Static	25%	75%	66%	56%	41%

Table 5. Summary of results with decision made based on a majority rule using ten scans.

Scenario	Data extraction	Collection Method	% data for training and regression	% data for testing	Neural Network Accuracy	Regression Model Accuracy	NDVI Model Accuracy
1	Systematic	Dynamic	50%	50%	91%	78%	60%
2	Systematic	Dynamic	25%	75%	90%	78%	59%
3	Systematic	Static	50%	50%	84%	71%	43%
4	Systematic	Static	25%	75%	75%	66%	40%
5	Consecutive	Dynamic	50%	50%	69%	54%	44%
6	Consecutive	Dynamic	25%	75%	79%	68%	55%
7	Consecutive	Static	50%	50%	51%	46%	37%
8	Consecutive	Static	25%	75%	68%	61%	43%

Linear regression

A multiple linear regression was performed for comparison with the neural network. A least squares fit model was created using the four spectral bands as the independent variables and N classification as the dependent variable. Model prediction accuracy was calculated using the same thresholds as discussed in the previous section. Figure 23 shows regression model N class prediction for scenario 1. The model appears to classify accurately using one of the dynamic data sets (right), but does not separate classes for the other data set(left). Tables 4 and 5 list results from regression model prediction. With decisions made every scan, prediction accuracy ranged from 56% to 75% for the eight different test scenarios. With decisions made every ten scans, the prediction accuracy range increased to 61% to 78%.

NDVI Index

NDVI is a commonly used index to evaluate plant health. Plant et al. (2000) suggests NDVI can be a fairly good predictor of higher nitrogen deficiencies in cotton. For these reasons, NDVI was also evaluated in this study. Average NDVI was calculated using data taken with the prototype system. Average NDVI had a weak to moderate correlation with nitrate and application rate, R^2=0.4987 and 0.6846 respectively (Figures 24 and 25). The higher correlation between NDVI and application rate was expected based on previous research (Sui, 1999). Based on prototype measurements taken on the cotton plots in this study, NDVI could not predict N status with a significant degree of accuracy. Using a least

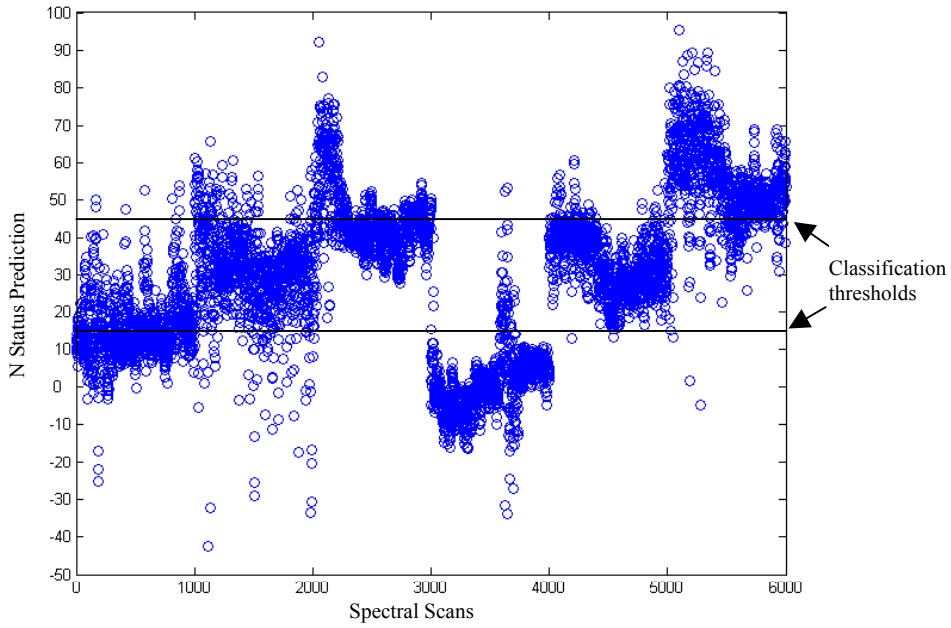


Figure 23. Regression prediction and thresholds for dynamically collected data with 50% for training and 50% for testing (scenario 1).

squares fit model, maximum NDVI prediction accuracy was 60%. Complete results for NDVI model tests are listed in Tables 4 and 5.

Summary

Reflected light energy in the red region had a good negative correlation with N classification. This is consistent with increasing chlorophyll absorption resulting from increasing N uptake (Wood et al., 1992). However, it is possible that this observed correlation is influenced in part by plant canopy density. As observed plant canopy density increased red reflected light could have possibly decreased due in part to some soil reflectance. Field test conditions were conducive to this possibility.

The three prediction methods were tested and compared over eight scenarios. Results show the neural network having the highest prediction accuracy for all eight scenarios (Tables 4 and 5). To examine and compare the distribution of misclassifications, a prediction error matrix was created for each of the three prediction methods (Tables 6, 7, and 8). Testing scenario 2 was used to create these matrices with a total of 9000 scans. Prediction error from the neural network is primarily due to misclassifying high and low N as medium N and misclassifying medium N as low and high N. Similarly, prediction error from regression is primarily due to misclassifying high and low N as medium N. Prediction error from NDVI is due to its tendency to over classify N status. This would suggest raising the classification thresholds during testing could increase NDVI accuracy.

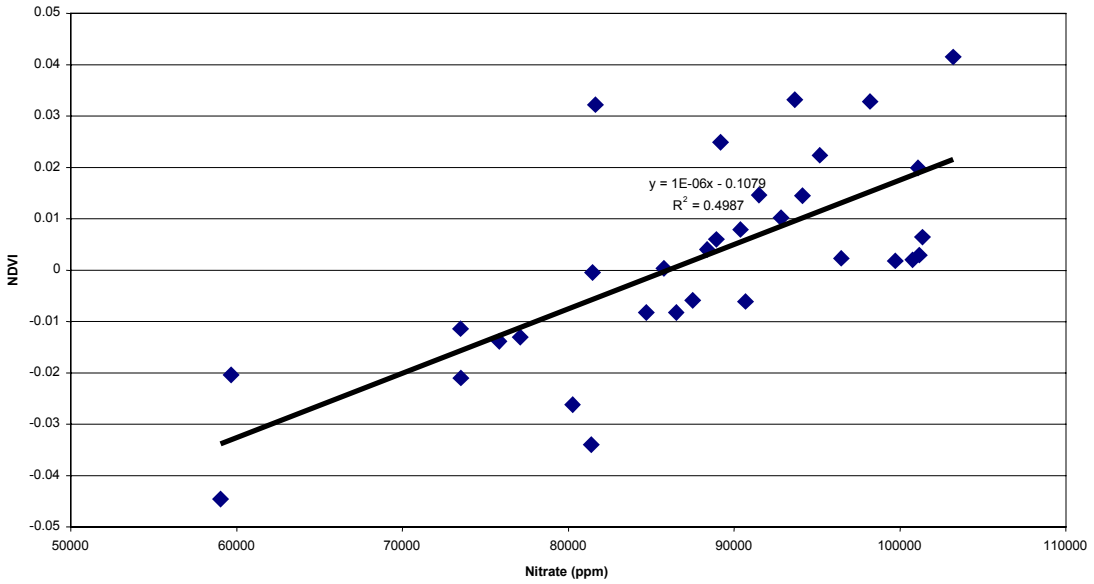


Figure 24. Average NDVI as a function of Nitrate (ppm).

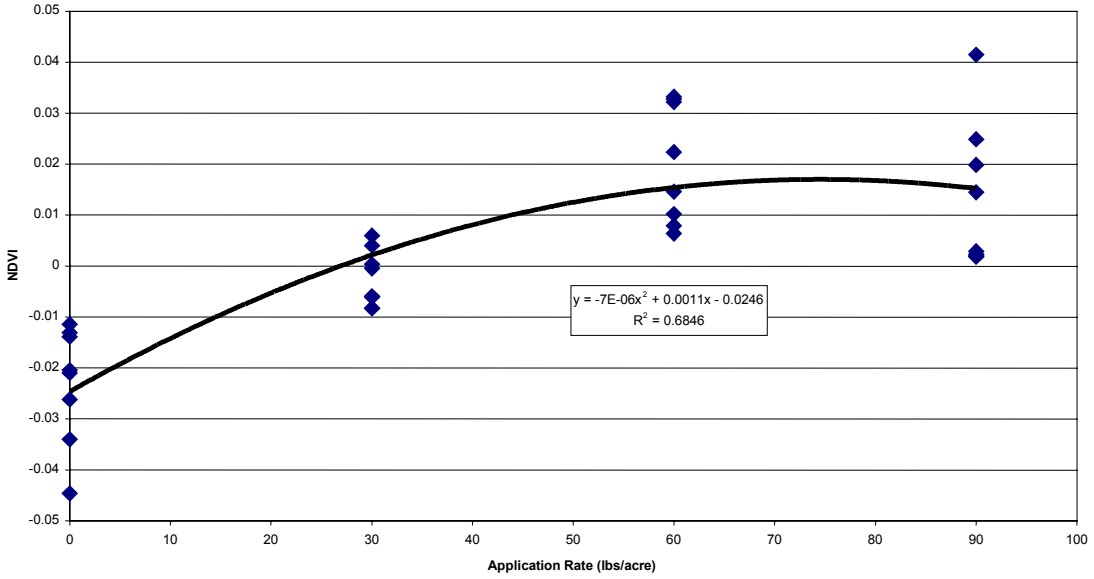


Figure 25. Average NDVI as a function of N application rate.

Table 6. Neural Network prediction error matrix.

		Predicted Classification		
		LOW	MED	HIGH
Actual Classification	LOW	2660	331	9
	MED	218	2555	227
	HIGH	10	305	2685

Table 7. Regression model prediction error matrix.

		Predicted Classification		
		LOW	MED	HIGH
Actual Classification	LOW	2237	748	15
	MED	121	2642	237
	HIGH	13	1151	1836

Table 8. NDVI model prediction error matrix.

		Predicted Classification		
		LOW	MED	HIGH
Actual Classification	LOW	1896	1022	82
	MED	44	2510	446
	HIGH	0	2160	840

CHAPTER V. SUMMARY AND CONCLUSIONS

Summary

A ground-based remote sensing system for diagnosing nitrogen status in cotton has been developed, prototyped and tested. The prototype system consists of three major sub-systems, a data acquisition and processing (DAP) system, a graphical user interface, and a multi-spectral sensing unit. The multi-spectral sensing unit projects four narrow wavebands of modulated light onto a target and measures the resulting reflected light intensity in each waveband. Wavebands are centered at 466, 540, 644, and 880 nm. The DAP system receives an analog signal from the sensing unit for data acquisition and/or processing.

The prototype system was tested on DP451 BRR cotton with four different N application rates. Based on a nitrate analysis, three nitrogen status classifications were identified: low, medium, and high. Reflected light energy in the red region produced the highest linear correlation with N status with a correlation coefficient of –0.7285. A feed forward neural network was trained to predict nitrogen status based on the four spectral measurements taken with the prototyped system. System performance was evaluated based on its ability to correctly classify N status. Results indicate that the system is capable of diagnosing nitrogen status in cotton with a high degree of accuracy. Using dynamically (≈1 mi/hr) acquired data, prediction accuracies greater than 91% were achieved when 50% of data was used for training and 50% used for testing. Accuracy decreased slightly to 90% when 25% of the data was used for training and 75% used for testing. Neural Network average accuracy proved to be slightly higher (>10%) than conventional linear models.

Conclusions

Based on testing performed during this study, the following conclusions were made:

- The prototype multi-spectral sensing unit developed in this study can successfully emit four narrow wavebands of light from a self-contained modulated illumination source and measure the resulting reflected light intensity from a cotton plant canopy independent of sunlight.
- Preliminary testing of the prototype system indicated the ability to very accurately distinguish between plant and soil.
- Based on tests from one year and one cotton variety the prototype system accurately classified N status in cotton.
- The prototyped system has the potential to learn non-linear relationships that have been found to exist in different cotton varieties and years (Sui, 1999).
- Utilizing neural networks, the prototype system outperformed the conventional NDVI and other linear techniques.
- System performance was potentially influenced by canopy density (i.e. soil in the field of view).

Recommendations

System Refinements

The sensing unit functioned as designed, although one problem encountered with using LEDs is the possibility of damaging them. LEDs can withstand much higher current than the manufacturer's specifications, especially if modulated. Care was taken not to exceed the limitations of the LEDs in this design. Although, it is recommended that future work investigates new LED technology as it becomes available. It is also suggested that higher luminance intensities (i.e. focusing LEDs onto a smaller target) or more LEDs may be beneficial in future designs. This refinement should increase sensitivity

The geometric shape of the photodiode and the focal length of the focusing lens created a field-of-view which was slightly larger than the projection beam. This design allowed light reflected from outside the field-of-view to strike the PCB. This may have illuminated the cavity between the photodiode and lens. It is unlikely but possible that this illuminated cavity could have reduced signal-to-noise ratio. If so it is recommended that the PCB and cavity be darkened to minimize this effect.

Additional Testing

This study was limited to one year and one cotton variety. Plant nitrate tests show less than desirable nitrogen stress in the study plots. Therefore, it is recommended that more high N stress plots of different varieties and years be acquired for future testing. It is also possible that this system could be highly successful in identifying weeds within crop rows. The prototype system has the potential to be used in numerous other applications

where spectral differences can be detected. It is hopeful that any future study can evaluate these possibilities as well as confirm current findings.

The possibility of unintentional detection of plant canopy density is a major concern for future testing. With light emission perpendicular to the soil, the sensing unit has the potential to measure plant and soil partial reflectance in sparse canopies. Orienting light projection at a 48 degree angle measured from vertical would place soil 50% farther away from the sensing unit. This will virtually eliminate the influence of soil reflectance in canopies with less density.

BIBLIOGRAPHY

BIBLIOGRAPHY

Beck, J. and T. Vyse. 1995. Structure and method usable for differentiating a plant form soil in a field. United States Patent No. 5389781

Benton M.E., R. Maples, R.D. May, W.N. Miley, W.E. Sabbe. 1979. A computerized system for cotton nitrate monitoring with program listings and descriptions. Fayetteville (AR): University of Arkansas Agricultural Experiment Station. Report Series 244.

Blackmer, T.M., J.S. Schepers, G.E. Varvel, and E.A. Walter-Shea. 1996. Nitrogen deficiency detection using reflected shortwave radiation from irrigated corn canopies. Agron. J. 88:1-5.

Borhan M.S, H. Gu, J. Lorenzen, and S. Panigrahi. 2001. Evaluation of multi-spectral imaging techniques to predict chlorophyll and nitrogen staus of potato leaves in the field. Presented at July 29-August 01, 2001 ASAE Annual International Meeting, Paper No. 011153. ASAE, 2950 Niles Road, St. Joseph, MI 49085-9659 USA.

Cybenko, G. 1989. Approximation by Superpositions of a Sigmoidal Function, *Mathematics of Control, Signals, and Systems*, 2, pp 303-314

Funahashi, K. 1989. On the Approximate Realization of Continous Mappings by Neural Networks, *Neural Networks*, 2, pp 183-192.

Haykin, S. 1994. *Neural Networks, A Comprehensive Foundation*. New York: Macmillan.

Hornick, K., M. Stinchcombe, and H. White, 1989. Multilayer Feedforward Networks are Universal Approximators, *Neural Networks*, 2, pp 359-366.

Hines, J.W. 1997. *MATLAB Supplement to Fuzzy and Neural Approaches in Engineering*. New York: John Wiley & Sons, Inc.

Kinter, M.L. and J. Beck. 1998. Detecting plants in a field by detecting a change in slope in a reflectance characteristic. United States Patent No. 5789741

Krugh, B.W., L. Bickham, and D. Miles. 2001. The solid-state chlorophyll meter: a novel instrument for rapidly and accurately determining the chlorophyll concentrations in seedling leaves. http://www.agron.missouri.edu/mnl/68/39krugh.html.

ORION. 1990. Model 93-07 Nitrate Electrode Instruction Manual. Model 90-02 Double Junction Reference Electrode Instruction Manual.

ORION. 1991. Laboratory Products Group Portable pH/ISE Meters Instruction Manual. Model 290A.

Plant, R.E., D.S. Munk, B.R. Roberts, R.L. Vargas, D.W. Rains, R.L., and Travis, R.B. Hutmacher. 2000. Relationships between remotely sensed reflectance data and cotton growth and yield. Trans. ASAE 43(3):535-546.

Read, J.J., L. Tarpley, J. M. McKinion, and K. R. Reddy. 2001 Narrow-Waveband Reflectance Ratios for Remote Estimation of Nitrogen Stress in Cotton Canopies. Unpublished research report. USDA-Agricultural Research Service, Crop Science Research Laboratory, P.O. Box 5367, Mississippi State, MS 39762

SAS® Institute Inc. 1989. SAS® Proprietary Software Release 6.12. TS020.

Scott, D.N.,and G.C. Trever. 2001. Plant discrimination based on leaf reflectance. ASAE Meeting Paper No. 01-1150. ASAE, 2950 Niles Road, St. Joseph, MI 49085-9659 USA.

Stone, M. L., J. B. Solie, R. W. Whitney, W. R. Raun, and H. L. Lees. 2001. Sensor for detection of nitrogen in winter wheat. http://bioen.okstate.edu/Home/mstone/N-Sens.htm.

Stone, M.L., J.B. Solie, W.R. Raun, R.W. Whitney, S.L. Taylor, and J.D. Ringer. 1997. Use of spectral reflectance for correcting in-season fertilizer nitrogen deficiencies in winter wheat. Trans. ASAE 39:1623-1631.

Stone, M. L. 1994. Embedded neural networks in real time controls. SAE paper no. 941067. SAE, Warrendale, PA.

Sui, R. 1999. A ground-based real-time remote sensing system for diagnosing nitrogen status in cotton plants. Ph.D. dissertation. The University of Tennessee.

Swain, P. H. and S. M. Davis. 1978. Remote Sensing. McGraw-Hill, Inc.

Tumbo S.D, D.G. Wagner, and P.H. Heinemann. 2001. On-the-go sensing of chlorophyll status in corn. ASAE Meeting Paper No. 01-1175. ASAE, 2950 Niles Road, St. Joseph, MI 49085-9659 USA.

The Math Works, Inc. 1995. Neural Network Toolbox.

University of Arkansas Soil Test Laboratory. 1991. Standard Procedure: Cotton petiole nitrate analysis. Procedure No. PL-0002.

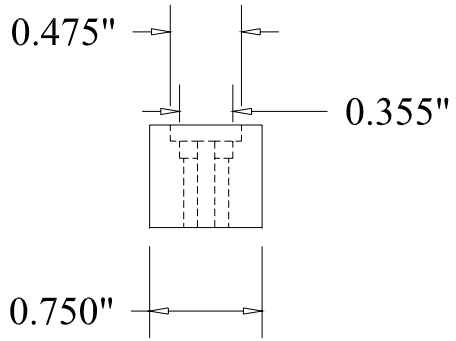
Wang, N., N. Zhang, F.E. Dowell, Y. Sun, and D.E. Peterson. 2001. Design of an optical weed sensor using plant spectral characteristics. Trans. ASAE 44(2):409-419.

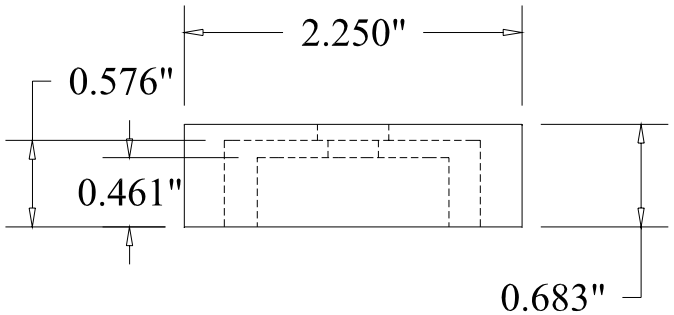
Wood, C.W., D.W. Reeves, R.R. Duffield and K.L. Edministen. 1992. Field chlorophyll measurements for evaluation of corn nitrogen status. Journal of Plant Nutrition. 15:487-500.

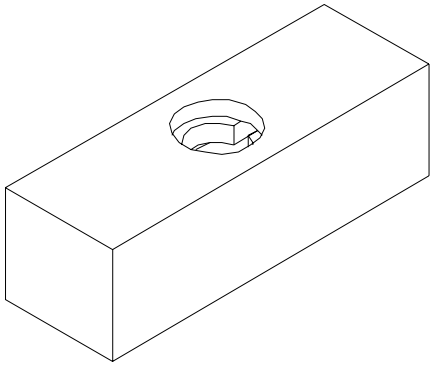
Wood, C.W., P. W. Tracy, D.W. Reeves, and K.L. Edministen. 1992. Determination of cotton nitrogen status with a hand-held chlorophyll meter. Journal of Plant Nutrition. 15(9):1435-1448.

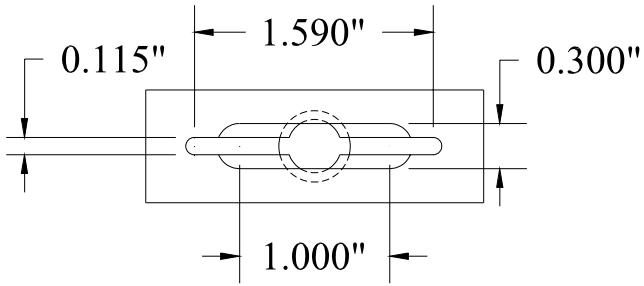
APPENDICIES

Appendix A Mechanical Drawings









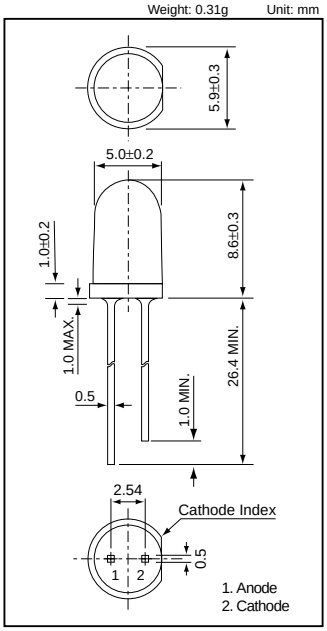
U.T. Ag. Eng. Dept	Title: Detector Lensholder	Drawn By: Christopher Whitten
Date: 5/16/01	Number Required: 1	Scale: Full Scale

Appendix B Electronic Device Specifications

SPECIFICATIONS FOR THE AND520HB BLUE LED

AND520HB
Ultra Bright LED Lamps: Type 3

Weight: 0.31g Unit: mm



AND520HB

GaN High Brightness Blue Light Emission

- 5 mm (T1-3/4) Package
- Peak wavelength (lp = 466nm) high bright emission
- All plastic mold type, clear colorless lens
- Low drive current: 1 to 20 mA DC
- Excellent On-Off contrast ratio
- Fast response time, capable of pulse operation
- High power intensity – suitable for Outdoor Message Signboards
- High reliability

Maximum Ratings (T_a = 25°C)

Characteristics	Symbol	Rating	Unit
Forward Current	I_F	30	mA
Reverse Voltage	V_R	5	V
Power Dissipation	P_D	120	mW
Operating Temperature Range	T_{Opr}	-40 to 85	C
Storage Temperature Range	T_{Sig}	-40 to 100	C

Electro-Optical Characteristics (T_a = 25°C)

Characteristics	Symbol	Test Condition	Minimum	Typical	Maximum	Unit
Forward Voltage	V_F	I_F = 20 mA	–	3.5	4.0	V
Reverse Current	I_R	V_R = 5V	–	–	10	µA
Luminous Intensity	I_V	I_F = 20 mA	–	1,400	–	mcd
Peak Emission Wavelength	I_P	I_F = 20 mA	–	466	–	nm
Spectral Line Half Width	ΔI	I_F = 20 mA	–	35	–	nm
Dominant Wavelength	Id	I_F = 20 mA	465	–	475	nm
Full Viewing Angle	q	I_V = 1/2 Peak	–	20	–	degree

Precaution

Please be careful of the following:

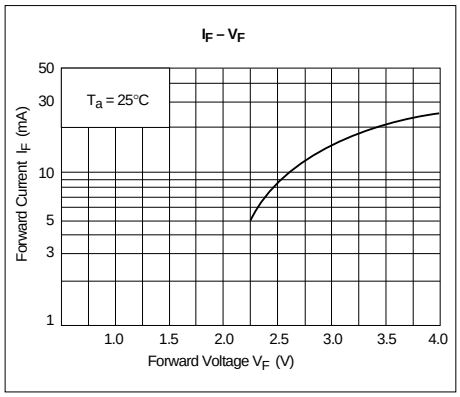
1. Soldering temperature: 260 C max.
   Soldering time: 5 sec. max.
   Soldering portion of lead: up to 1.6 mm from the body of the device
2. The lead can be formed up to 5 mm from the body of the device without forming stress.
   Soldering should be performed after the lead forming.
3. Absolute secure counter measures against static electricity and surge should be taken when handling these products. It is recommended to use wrist band or antistatic gloves when handling these LEDs.

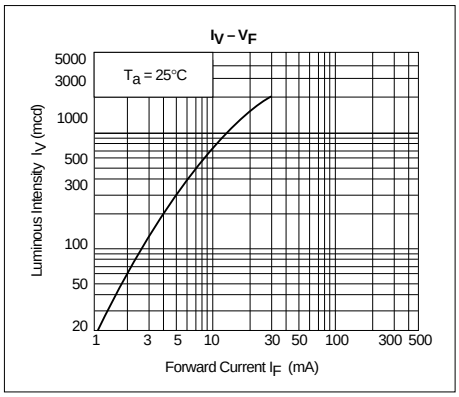
Purdy Electronics Corporation • 720 Palomar Avenue • Sunnyvale, CA 94086
Tel: 408.523.8200 • Fax: 408.733.1287 • email@purdyelectronics.com • www.purdyelectronics.com 6-1-99

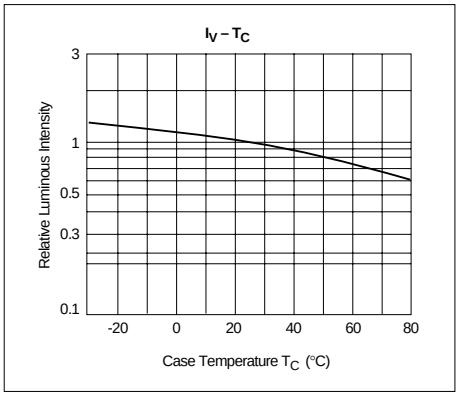
SPECIFICATIONS FOR THE AND520HB BLUE LED (CONTINUED).

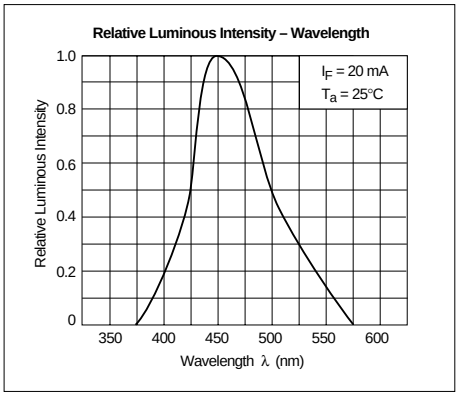
AND520HB

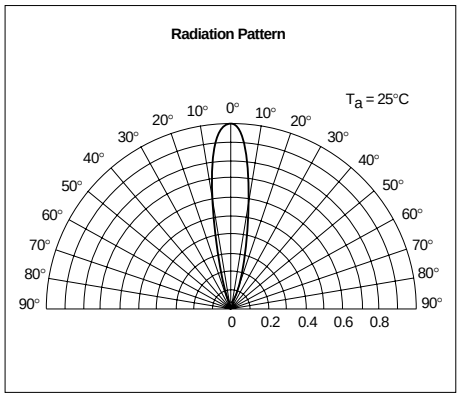
GaN High Brightness Blue Light Emission — **Ultra Bright LED Lamps: Type 3**

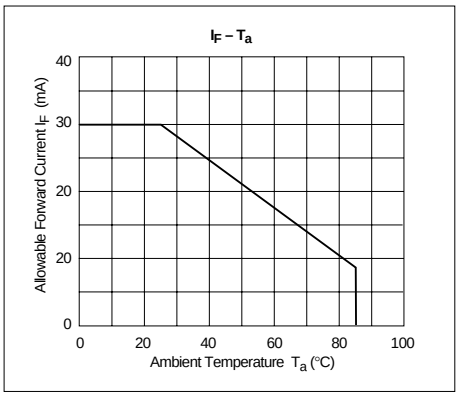










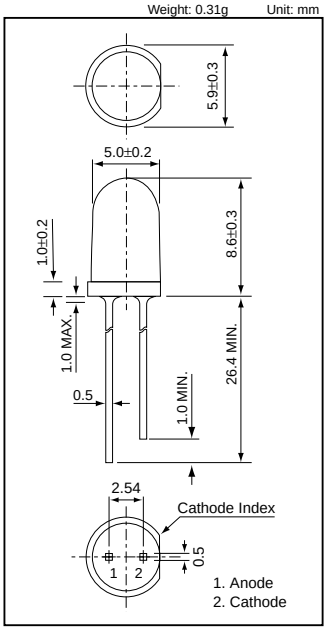


Purdy Electronics Corporation • 720 Palomar Avenue • Sunnyvale, CA 94086
Tel: 408.523.8200 • Fax: 408.733.1287 • email@purdyelectronics.com • www.purdyelectronics.com

6-1-99

SPECIFICATIONS FOR THE AND520HG GREEN LED.

Weight: 0.31g Unit: mm



AND520HG

GaN High Brightness Green Light Emission

- 5 mm (T1-3/4) Package
- Peak wavelength (lp = 540nm) high bright emission
- All plastic mold type, clear colorless lens
- Low drive current: 1 to 20 mA DC
- Excellent On-Off contrast ratio
- Fast response time, capable of pulse operation
- High power intensity – suitable for Outdoor Message Signboards
- High reliability

Maximum Ratings (T_a = 25°C)

Characteristics	Symbol	Rating	Unit
Forward Current	I_F	30	mA
Reverse Voltage	V_R	5	V
Power Dissipation	P_D	120	mW
Operating Temperature Range	T_{Opr}	-40 to 85	C
Storage Temperature Range	T_{Sig}	-40 to 100	C

Electro-Optical Characteristics (T_a = 25°C)

Characteristics	Symbol	Test Condition	Minimum	Typical	Maximum	Unit
Forward Voltage	V_F	I_F = 20 mA	–	3.5	4.0	V
Reverse Current	I_R	V_R = 5V	–	–	10	µA
Luminous Intensity	I_V	I_F = 20 mA	–	5,000		mcd
Peak Emission Wavelength	I_P	I_F = 20 mA	–	540	–	nm
Spectral Line Half Width	ΔI	I_F = 20 mA	–	45	–	nm
Dominant Wavelength	Id	I_F = 20 mA	520	–	550	nm
Full Viewing Angle	q	I_V = 1/2 Peak	–	20	–	degree

Precaution

Please be careful of the following:

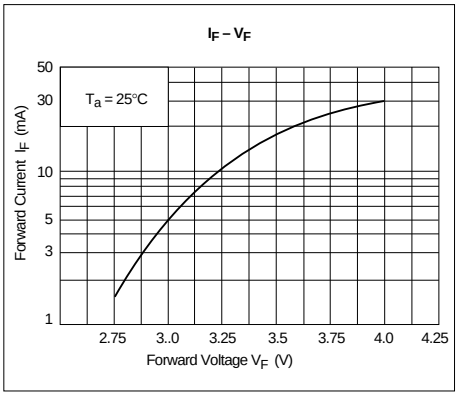
1. Soldering temperature: 260 C max.
   Soldering time: 5 sec. max.
   Soldering portion of lead: up to 1.6 mm from the body of the device
2. The lead can be formed up to 5 mm from the body of the device without forming stress.
   Soldering should be performed after the lead forming.
3. Absolute secure counter measures against static electricity and surge should be taken when handling these products. It is recommended to use wrist band or antistatic gloves when handling these LEDs.

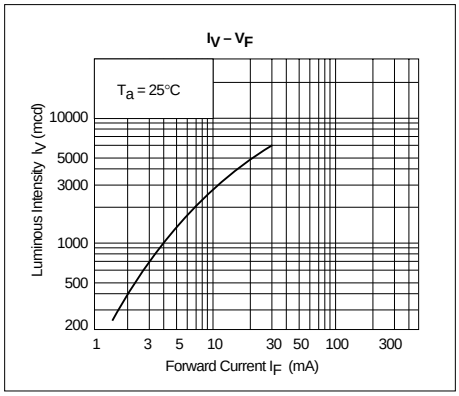
Purdy Electronics Corporation • 720 Palomar Avenue • Sunnyvale, CA 94086
Tel: 408.523.8200 • Fax: 408.733.1287 • email@purdyelectronics.com • www.purdyelectronics.com 6-1-99

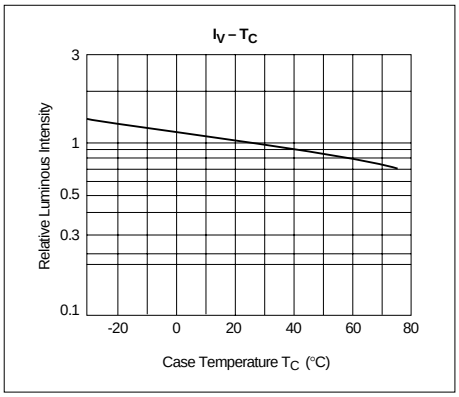
SPECIFICATIONS FOR THE AND520HG GREEN LED (CONTINUED).

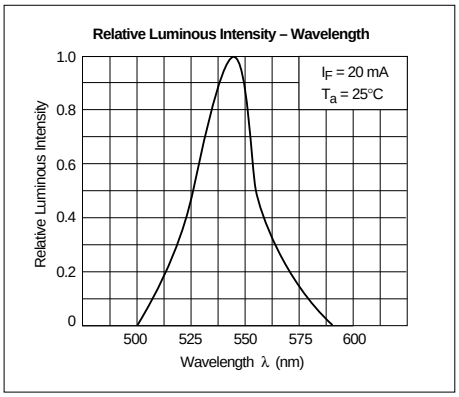
AND520HG

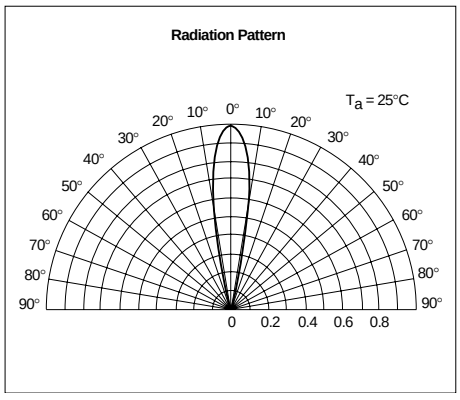
GaN High Brightness Green Light Emission **Ultra Bright LED Lamps: Type 3**

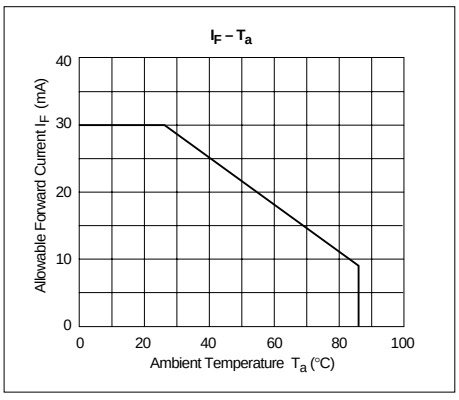










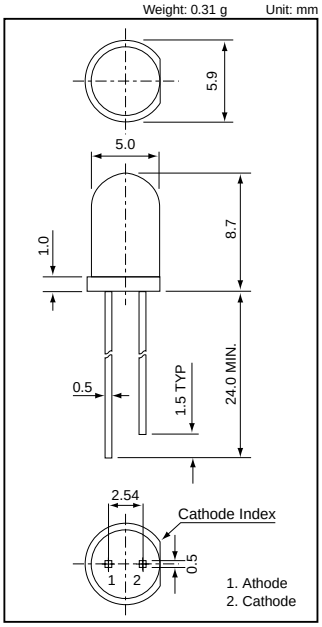


Purdy Electronics Corporation • 720 Palomar Avenue • Sunnyvale, CA 94086
Tel: 408.523.8200 • Fax: 408.733.1287 • email@purdyelectronics.com • www.purdyelectronics.com

6-1-99

SPECIFICATIONS FOR THE AND157HRP RED LED.

Weight: 0.31 g Unit: mm



AND157HRP

InGaAlP High Brightness Red Light Emission
T-1 3/4 Package (5 mm)

Features

- Peak wavelength (λp = 644 nm) high bright emission
- All plastic mold type, clear colorless lens
- Low drive current: 1 to 20 mA DC
- Excellent On-Off contrast ratio
- Fast response time, capable of pulse operation
- High power luminous intensity
- Suitable for Outdoor Message Signboards
- High reliability, storage temperature -40 to +20°C

Maximum Ratings (T_a = 25°C)

Characteristics	Symbol	Rating	Unit
Forward Current	I_F	30	mA
Reverse Voltage	V_R	4	V
Power Dissipation	P_D	100	mW
Operating Temperature Range	T_{Opr}	-25 to 85	°C
Storage Temperature Range	T_{Stg}	-25 to 120	°C

Electro-Optical Characteristics (T_a = 25°C)

Characteristics	Symbol	Test Condition	Minimum	Typical	Maximum	Unit
Forward Voltage	V_F	I_F = 20 mA	–	2.0	2.4	V
Reverse Current	I_R	V_R = 4 V	–	–	50	µA
Luminous Intensity	I_V	I_F = 20 mA	700	1,800	–	mcd
Peak Emission Wavelength	I_P	I_F = 20 mA	–	644	–	nm
Spectral Line Half Width	Δλ	I_F = 20 mA	–	15	–	nm
Dominant Wavelength	λd	I_F = 20 mA	–	630	–	nm
Full Viewing Angle	θ	I_V = 1/2 Peak	–	20	–	degree

Precaution

Please be careful of the following:

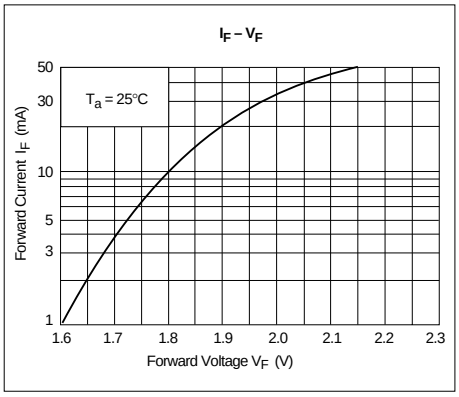
1. Soldering temperature: 260°C max
   Soldering time: 5 sec. max
   Soldering portion of lead: up to 1.6 mm from the body of the device
2. The lead can be formed up to 5 mm from the body of the device without forming stress.
   Soldering should be performed after the lead forming.

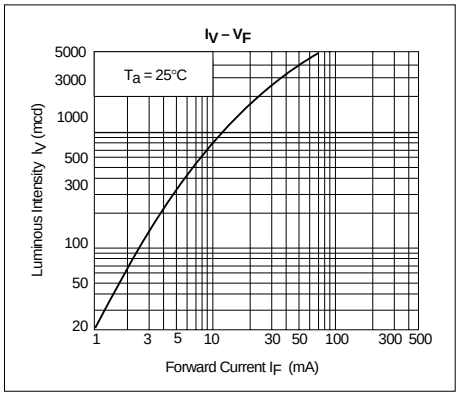
Purdy Electronics Corporation • 720 Palomar Avenue • Sunnyvale, CA 94086
Tel: 408.523.8200 • Fax: 408.733.1287 • email@purdyelectronics.com • www.purdyelectronics.com 6-1-99

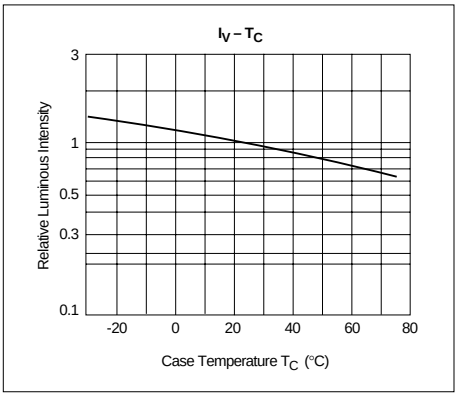
SPECIFICATIONS FOR THE AND157HRP RED LED (CONTINUED).

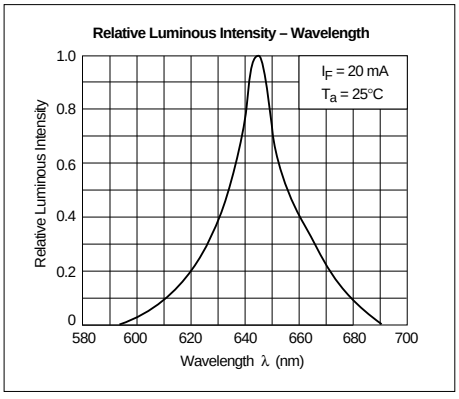
AND157HRP

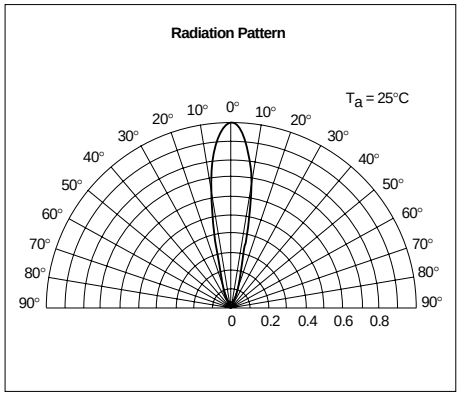
InGaAlP High Brightness Red Light Emission **Ultra Bright LED Lamps: Type 3**

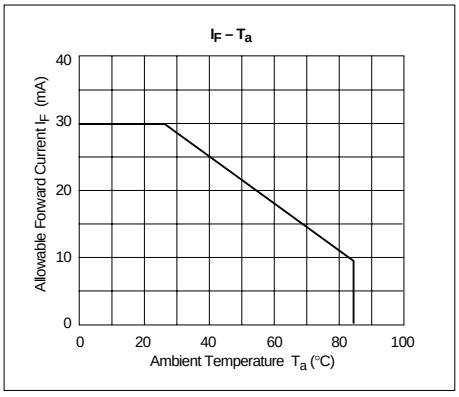












Purdy Electronics Corporation • 720 Palomar Avenue • Sunnyvale, CA 94086
Tel: 408.523.8200 • Fax: 408.733.1287 • email@purdyelectronics.com • www.purdyelectronics.com 6-1-99

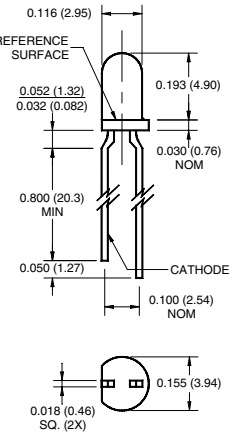
SPECIFICATIONS FOR THE QEC123 INFRARED LED.

FAIRCHILD SEMICONDUCTOR®

PLASTIC INFRARED LIGHT EMITTING DIODE

QEC121 **QEC122** **QEC123**

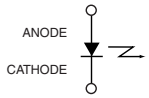
PACKAGE DIMENSIONS



NOTES:
1. Dimensions are in inches (millimeters)
2. Tolerance of ± .010 (.25) on all non nominal dimensions unless otherwise specified.



SCHEMATIC



DESCRIPTION

The QEC12X is an 880 nm AlGaAs LED encapsulated in a clear purple tinted, plastic T-1 package.

FEATURES

- λ= 880 nm
- Chip material = AlGaAs
- Package type: T-1 (3mm lens diameter)
- Matched Photosensor: QSC112/113/114
- Narrow Emission Angle, 16°
- High Output Power
- Package material and color: Clear, purple tinted, plastic

© 2001 Fairchild Semiconductor Corporation

SPECIFICATIONS FOR THE QEC123 INFRARED LED (CONTINUED).

FAIRCHILD SEMICONDUCTOR®

PLASTIC INFRARED LIGHT EMITTING DIODE

QEC121 QEC122 QEC123

ABSOLUTE MAXIMUM RATINGS (T_A = 25°C unless otherwise specified)

Parameter	Symbol	Rating	Unit
Operating Temperature	T_{OPR}	-40 to +100	°C
Storage Temperature	T_{STG}	-40 to +100	°C
Soldering Temperature (Iron)(2,3,4)	T_{SOL-I}	240 for 5 sec	°C
Soldering Temperature (Flow)(2,3)	T_{SOL-F}	260 for 10 sec	°C
Continuous Forward Current	I_F	50	mA
Reverse Voltage	V_R	5	V
Power Dissipation(1)	P_D	100	mW

NOTES

1. Derate power dissipation linearly 1.33 mW/°C above 25°C.
2. RMA flux is recommended.
3. Methanol or isopropyl alcohols are recommended as cleaning agents.
4. Soldering iron 1/16" (1.6mm) minimum from housing.

ELECTRICAL / OPTICAL CHARACTERISTICS (T_A = 25°C)

PARAMETER	TEST CONDITIONS	SYMBOL	MIN	TYP	MAX	UNITS
Peak Emission Wavelength	I_F = 100 mA	λ_{PE}	—	880	—	nm
Emission Angle	I_F = 100 mA	$2\Theta_{1/2}$	—	16	—	Deg.
Forward Voltage	I_F = 100 mA, tp = 20 ms	V_F	—	—	1.7	V
Reverse Current	V_R = 5 V	I_R	—	—	10	µA
Radiant IntensityQEC121	I_F = 100 mA, tp = 20 ms	I_E	14	—	—	mW/sr
Radiant IntensityQEC122	I_F = 100 mA, tp = 20 ms	I_E	27	—	94	mW/sr
Radiant IntensityQEC123	I_F = 100 mA, tp = 20 ms	I_E	39	—	—	mW/sr
Rise Time	I_F = 100 mA	t_r	—	800	—	ns
Fall Time		t_f	—	800	—	ns

SPECIFICATIONS FOR THE QEC123 INFRARED LED (CONTINUED).

FAIRCHILD SEMICONDUCTOR®

PLASTIC INFRARED LIGHT EMITTING DIODE

QEC121 QEC122 QEC123

Fig.1 Normalized Radiant Intensity vs. Forward Current

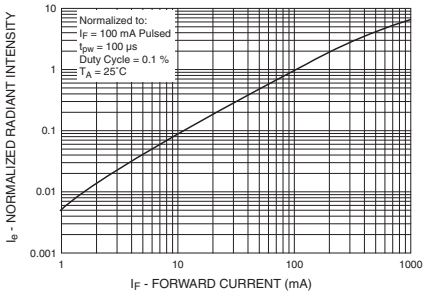


Fig.2 Coupling Characteristics of QEC12X And QSC11X

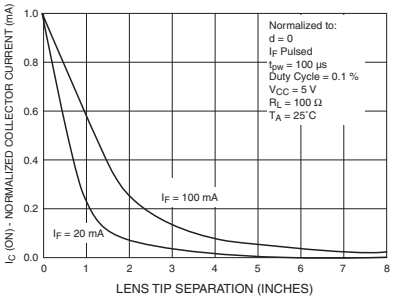


Fig.3 Forward Voltage vs. Ambient Temperature

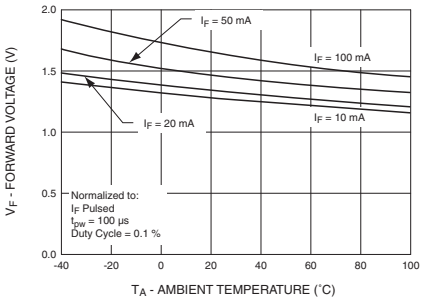


Fig. 4 Normalized Radiant Intensity vs. Wavelength

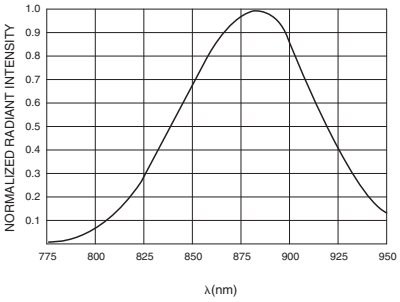
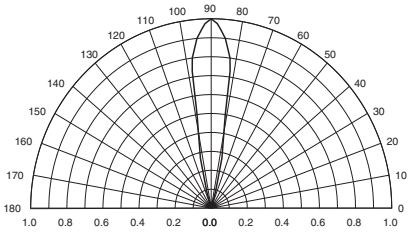


Fig. 5 Radiation Diagram

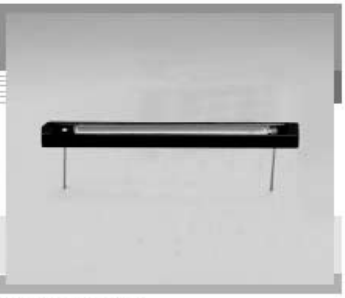


SPECIFICATIONS FOR THE S2551 PHOTODIODE.

PHOTODIODE

Si photodiode
S2551

For visible to infrared precision photometry



S2551 is a Si photodiode having a long active area of 1.2 × 29.1 mm, designed for visible to infrared precision photometry.

Features

- Long, narrow active area: 1.2 × 29.1 mm
- High sensitivity
- Low capacitance

Applications

- Analytical instruments
- Optical measurement equipment

■ Absolute maximum ratings

Parameter	Symbol	Value	Unit
Reverse voltage	V_R Max.	30	V
Operating temperature	Topr	-20 to +60	°C
Storage temperature	Tstg	-20 to +80	°C

■ Electrical and optical characteristics (Ta=25 °C)

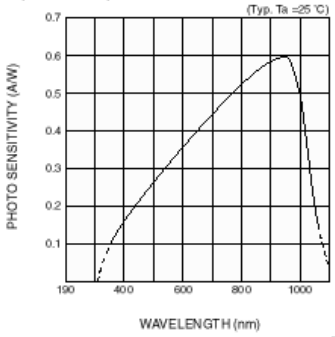
Parameter	Symbol	Condition	Min.	Typ.	Max.	Unit
Spectral response range	λ		-	320 to 1060	-	nm
Peak sensitivity wavelength	λp		-	920	-	nm
Photo sensitivity	S	λ=λp	-	0.6	-	A/W
		λ=663 nm	-	0.37	-	A/W
Short circuit current	Isc	100 lx	24	30	-	μA
Dark current	I_D	V_R=10 mV	-	-	1	nA
Temperature coefficient of I_D	T_{CID}		-	1.15	-	times/°C
Rise time	tr	V_R=0 V, R_L=1 kΩ	-	0.6	-	μs
Terminal capacitance	Ct	V_R=0 V, f=10 kHz	-	350	-	pF
Shunt resistance	Rsh	V_R=10 mV	0.01	0.03	-	GΩ
Noise equivalent power	NEP		-	3.9×10^{-14}	-	$W/Hz^{1/2}$

SOLID STATE DIVISION

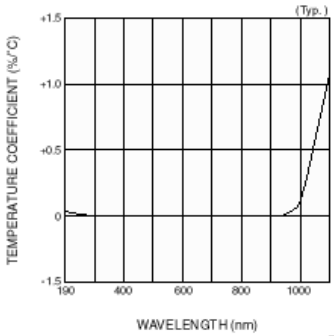
HAMAMATSU

SPECIFICATIONS FOR THE S2551 PHOTODIODE (CONTINUED).

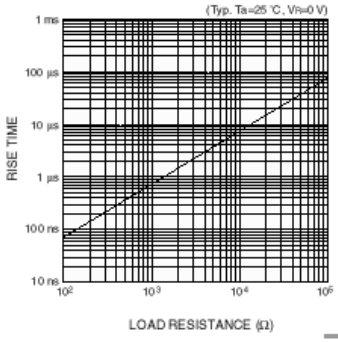
■ Spectral response



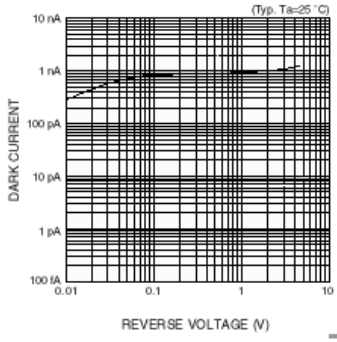
■ Photo sensitivity temperature characteristic



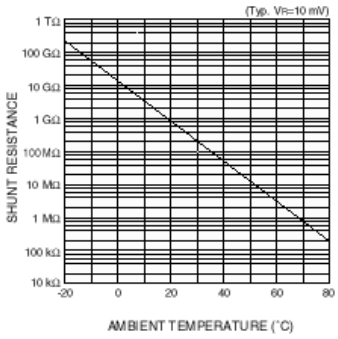
■ Rise time vs. load resistance



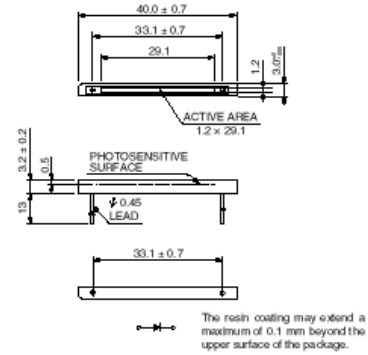
■ Dark current vs. reverse voltage



■ Shunt resistance vs. ambient temperature



■ Dimensional outline (unit: mm)



HAMAMATSU Information furnished by HAMAMATSU is believed to be reliable. However, no responsibility is assumed for possible inaccuracies or omissions. Specifications are subject to change without notice. No patent rights are granted to any of the circuits described herein. ©2001 Hamamatsu Photonics K.K.

HAMAMATSU PHOTONICS K.K., Solid State Division
1126-1 Ichino-cho, Hamamatsu City, 435-8558 Japan, Telephone: (81) 053-434-3311, Fax: (81) 053-434-5184, http://www.hamamatsu.com
U.S.A.: Hamamatsu Corporation: 360 Foothill Road, P.O.Box 6910, Bridgewater, N.J. 08807-0910, U.S.A., Telephone: (1) 908-231-0960, Fax: (1) 908-231-1218
Germany: Hamamatsu Photonics Deutschland GmbH: Arzbergerstr. 10, D-82211 Herrsching am Ammersee, Germany, Telephone: (49) 08152-3750, Fax: (49) 08152-2658
France: Hamamatsu Photonics France S.A.R.L.: 8, Rue du Saule Trapu, Parc du Moulin de Massy, 91882 Massy Cedex, France, Telephone: 33-(1) 69 53 71 00, Fax: 33-(1) 69 53 71 10
United Kingdom: Hamamatsu Photonics UK Limited: 2 Howard Court, 10 Tewin Road, Welwyn Garden City, Hertfordshire AL7 1BW, United Kingdom, Telephone: (44) 1707-294888, Fax: (44) 1707-325777
North Europe: Hamamatsu Photonics Norden AB: Smidesvägen 12, SE-171 41 Solna, Sweden, Telephone: (46) 8-509-031-00, Fax: (46) 8-509-031-01
Italy: Hamamatsu Photonics Italia S.R.L.: Strada della Moia, 1/E, 20020 Arese, (Milano), Italy, Telephone: (39) 02-935-81-733, Fax: (39) 02-935-81-741

Cat. No. KSPD1027E01
Mar. 2001 DN

Appendix C Data Acquisition Program

```
'================================================================
================

' Program controls LED's, reads A/D and then writes Spectral Reflectance
' Measurements to a file.
' Christopher Whitten 7/10/01
' Agricultural and Biosystems Engineering Department
' The University of Tennessee

'================================================================
================

Const BoardNum% = 0             ' Board number
Const PortNum% = AUXPORT        ' set port type to auxilliary

Private Sub cmdStartConvert_Click()
  Recording.Visible = 1
  cmdStartConvert.Visible = 0
  cmdStopConvert.Visible = 1
  cmdStopConvert.Default = 1
  tmrConvert.Enabled = -1
  filename = filename.Text

End Sub
```

```
Private Sub cmdStopConvert_Click()
  tmrConvert.Enabled = 0

  ULStat% = cbDOut%(BoardNum, PortNum%, 3)
   If ULStat% <> 0 Then Stop

End Sub

Private Sub Form_Load()

  ' declare revision level of Universal Library

   ULStat% = cbDeclareRevision(4) 'CURRENTREVNUM)

  ' Initiate error handling
  '  activating error handling will trap errors like
  '  bad channel numbers and non-configured conditions.
  '  Parameters:
  '    PRINTALL    :all warnings and errors encountered will be printed
  '    DONTSTOP    :if an error is encountered, the program will not stop,
  '                 errors must be handled locally

  ULStat% = cbErrHandling%(PRINTALL, DONTSTOP)
```

```
  If ULStat% <> 0 Then Stop

  ' If cbErrHandling% is set for STOPALL or STOPFATAL during the program
  ' design stage, Visual Basic will be unloaded when an error is encountered.
  ' We suggest trapping errors locally until the program is ready for compiling
  ' to avoid losing unsaved data during program design.  This can be done by
  ' setting cbErrHandling options as above and checking the value of ULStat%
  ' after a call to the library. If it is not equal to 0, an error has occurred.

End Sub
Private Sub Pause_Click()
End Sub
Private Sub Recording_Click()
End Sub

Private Sub tmrConvert_Timer()

Dim x(0 To 3)

 ' Collect the data with cbAIn%()

  '  Parameters:
  '    BoardNum%    :the number used by CB.CFG to describe this board
```

```
'   Chan%       :the input channel number
'   Gain%       :the gain for the board.
'   DataValue%  :the name for the value collected

Gain% = UNI10VOLTS          ' set the gain
Chan% = 0                   ' set input channel

For color% = 0 To 3

 ULStat% = cbDOut%(BoardNum, PortNum%, color%)
 If ULStat% <> 0 Then Stop

For stab = 1 To 10000
Next stab
'For i% = 1 To 9

 ULStat% = cbAIn%(BoardNum%, Chan%, Gain%, DataValue%)
 If ULStat% = 30 Then MsgBox "Change the Gain% argument to one supported
by this board.", 0, "Unsupported Gain"
 If ULStat% <> 0 Then Stop

'  ULStat% = cbToEngUnits(BoardNum%, Gain%, DataValue%, EngUnits!)
 ' If ULStat% <> 0 Then Stop
```

```
'  lblShowData.Caption = Format$(DataValue%, "0")   ' print the counts
'   lblShowVolts.Caption = Format$(EngUnits!, "0.000") + " Volts"   ' print the
voltage
'If color = 1 Then
'    IR = Format$(EngUnits!, "0.000")
'ElseIf color = 2 Then
'   Blue = Format$(EngUnits!, "0.000")
'ElseIf color = 3 Then
'    Red = Format$(EngUnits!, "0.000")
'Else
'    Green = Format$(EngUnits!, "0.000")
'End If
't(i) = DataValue%        'Format$(EngUnits!, "0.000")
'Next i%
x(color%) = DataValue%
Next color%
Open filename & ".txt" For Append As #1    ' Open file for output.
Print #1, x(0), x(1), x(2), x(3)
Close #1    ' Close file.

 End Sub
```

Appendix D Matlab Post-Processing Programs

MATLAB CODE FOR *INPUT_RAW_DATA.M*

%This program reads data save in text files.

```
% x:input patterns. Each row is one scan. Each column is one waveband

% The 1st column of x: reflected light centered at 466 nm (BLUE)
      %
% The 2nd column of x: reflected light centered at 540 nm (RED)
      %
% The 3rd column of x: reflected light centered at 644 nm (GREEN)
      %
% The 4th column of x: reflected light centered at 880 nm (NIR)
      %
                              %
% y:Outputs. Each row is corresponding to defines N status
%classification .                                  %
%                                                          %
% There are three outputs:
%0 0 1: Nitrogen status is low (N application rate of 0 lbs/ac ).
%0 1 0: Nitrogen status is medium (N application rate of 30 lbs/ac ).
%1 0 0: Nitrogen status is high (N application rates of 60 and 90
%lbs/ac ).        %



x=[];
y=[];


for rate=0:30:60                    %looping through application rates
arate=num2str(rate);
for i=1:4                           %looping through plot replications
   t=num2str(i);
   a=strcat((arate),('-'),(t),('-'),(plo),('-'),(typ),('.txt'));
   a=char(a);

   [blue,red,green,ir] = textread(a,'%f %f %f %f');
   t=blue+red+green+ir;
   in=[(blue),(red),(green),(ir)];
   [r,c]=size(in);

   x=[x; in];

   if rate==0                        %growing the output matrix
      ys=[0 0 1];
      y=[y; (repmat(ys, [r,1]))];
   elseif rate==30
      ys=[0 1 0];
      y=[y; (repmat(ys, [r,1]))];
   elseif rate==60
      ys=[1 0 0];
```

```
      y=[y; (repmat(ys, [r,1]))];
   elseif rate==90
      ys=[1 0 0];
      y=[y; (repmat(ys, [r,1]))];
   end


end
end
b=[60 30 0]';
y=y*b;
```

MATLAB CODE FOR *SAVE_DATA.M*

%This program saves data read with *input_raw_data.m*.

```
clear;
typ='s';
plo='a';
inputrawdata;
filename=strcat((plo),(typ));
eval(['save ',filename,' x y ']);


clear;
typ='s';
plo='b';
inputrawdata;
filename=strcat((plo),(typ));
eval(['save ',filename,' x y ']);


clear;
typ='d';
plo='a';
inputrawdata;
filename=strcat((plo),(typ));
eval(['save ',filename,' x y ']);


clear;
typ='d';
plo='b';
inputrawdata;
filename=strcat((plo),(typ));
eval(['save ',filename,' x y ']);
```

MATLAB CODE FOR *EXTRACT.M*

```
%This program provides training and test data with equal representation
%for each of the three N classifications

%extract dynamic data

load bd                                          %load first half of dynamic data
thresfilter
ind0=find(y==0);
ind30=find(y==30);
ind60=find(y==60);
[a,q]=size(ind0);
[b,q]=size(ind30);
[c,q]=size(ind60);
s=min([a,b,c]);
xx=x((ind0(1:1:2000)),:);
xx(2001:4000,1:4)=x((ind30(1:1:2000)),:);
xx(4001:6000,1:4)=x((ind60(1:1:2000)),:);
yy=y((ind0(1:1:2000)),:);
yy(2001:4000)=y((ind30(1:1:2000)));
yy(4001:6000)=y((ind60(1:1:2000)));

x=xx;
y=yy;
save o50train x y;                    %save dynamic consecutive(row end b) 50%


load ad                                          %load second half of dynamic data
thresfilter
ind0=find(y==0);
ind30=find(y==30);
ind60=find(y==60);
[a,q]=size(ind0);
[b,q]=size(ind30);
[c,q]=size(ind60);
s=min([a,b,c]);
xx=x((ind0(1:1:2000)),:);
xx(2001:4000,1:4)=x((ind30(1:1:2000)),:);
xx(4001:6000,1:4)=x((ind60(1:1:2000)),:);
yy=y((ind0(1:1:2000)),:);
yy(2001:4000)=y((ind30(1:1:2000)));
yy(4001:6000)=y((ind60(1:1:2000)));
```

```
x=xx;
y=yy;
save o50test x y;                    %save dynamic consecutive(row end a) 50%

clear

load o50train
xx=x;
yy=y;
load o50test
x(6001:12000,1:4)=xx;
y(6001:12000)=yy;

xtrain=x(1:2:12000,1:4);
ytrain=y(1:2:12000);
xtest=x(2:2:12000,1:4);
ytest=y(2:2:12000);

x=xtrain;
y=ytrain;
save r50train x y                    %save dynamic systematic 50%

x=xtest;
y=ytest;
save r50test x y                     %save dynamic systematic remaining 50%


clear
load o50train
xx=x;
yy=y;
load o50test
x(6001:12000,1:4)=xx;
y(6001:12000)=yy;
A=[1 0 1 1];
b=repmat(A,1,3000);
xtrain=x((find(b==0)),1:4);
ytrain=y(find(b==0));

xtest=x((find(b)),1:4);
ytest=y(find(b));


x=xtrain;
y=ytrain;
```

```
save r25train x y                                   %save dynamic systematic 25%

x=xtest;
y=ytest;
save r75test x y                                    %save dynamic systematic remaining 75%


clear
load o50train
xtrain=x(1:2:6000,1:4);
ytrain=y(1:2:6000);
xtest=x(2:2:6000,1:4);
ytest=y(2:2:6000);

load o50test
xtest(3001:9000,1:4)=x;
ytest(3001:9000)=y;

x=xtrain;
y=ytrain;
save o25train x y;                                  %save dynamic consecutive(row end b) 25%

x=xtest;
y=ytest;
save o75test x y;                                   %save dynamic consecutive(row end a) 75%

%extract static data

load bs                                             %load first half of static data
thresfilter
ind0=find(y==0);
ind30=find(y==30);
ind60=find(y==60);
[a,q]=size(ind0);
[b,q]=size(ind30);
[c,q]=size(ind60);
s=min([a,b,c]);
xx=x((ind0(1:1:500)),:);
xx(501:1000,1:4)=x((ind30(1:1:500)),:);
xx(1001:1500,1:4)=x((ind60(1:1:500)),:);
yy=y((ind0(1:1:500)),:);
yy(501:1000)=y((ind30(1:1:500)));
yy(1001:1500)=y((ind60(1:1:500)));

x=xx;
```

```
y=yy;
save os50train x y;                    %save static consecutive(row end b) 50%


load as                                %load second half of dynamic data
thresfilter
ind0=find(y==0);
ind30=find(y==30);
ind60=find(y==60);
[a,q]=size(ind0);
[b,q]=size(ind30);
[c,q]=size(ind60);
s=min([a,b,c]);
xx=x((ind0(1:1:500)),:);
xx(501:1000,1:4)=x((ind30(1:1:500)),:);
xx(1001:1500,1:4)=x((ind60(1:1:500)),:);
yy=y((ind0(1:1:500)),:);
yy(501:1000)=y((ind30(1:1:500)));
yy(1001:1500)=y((ind60(1:1:500)));

x=xx;
y=yy;
save os50test x y;                     %save static consecutive(row end a) 50%

clear

load os50train
xx=x;
yy=y;
load os50test
x(1501:3000,1:4)=xx;
y(1501:3000)=yy;

xtrain=x(1:2:3000,1:4);
ytrain=y(1:2:3000);
xtest=x(2:2:3000,1:4);
ytest=y(2:2:3000);

x=xtrain;
y=ytrain;
save rs50train x y                     %save static systematic 50%

x=xtest;
y=ytest;
save rs50test x y                      %save static systematic remaining 50%
```

```
clear
load os50train
xx=x;
yy=y;
load os50test
x(1501:3000,1:4)=xx;
y(1501:3000)=yy;
A=[1 0 1 1];
b=repmat(A,1,750);
xtrain=x((find(b==0)),1:4);
ytrain=y(find(b==0));

xtest=x((find(b)),1:4);
ytest=y(find(b));


x=xtrain;
y=ytrain;
save rs25train x y                          %save static systematic 25%

x=xtest;
y=ytest;
save rs75test x y                       %save static systematic remaining 75%


clear
load os50train
xtrain=x(1:2:1500,1:4);
ytrain=y(1:2:1500);
xtest=x(2:2:1500,1:4);
ytest=y(2:2:1500);

load os50test
xtest(751:2250,1:4)=x;
ytest(751:2250)=y;

x=xtrain;
y=ytrain;
save os25train x y;                     %save static consecutive(row end b) 25%

x=xtest;
y=ytest;
save os75test x y;                      %save static consecutive(row end a) 75%
```

MATLAB CODE FOR *AGRIEYE.M*

```
%This program trains a feed forward NN using given input/output pairs using
%lmtrain


vecfile = input('Enter filename of training data: ','s');
numhid = input('How many neurons in the hidden layer? ');

sel1 = input('Sigmoid, Tansigmoid, or Linear for hidden layer? [s,t,l]: ','s');
sel2 = input('Sigmoid, Tansigmoid, or Linear for output layer? [s,t,l]: ','s');

sc=input('Input/Output Scaling Type MCUV=m,linear=l,none=n?[m,l,n]:','s');

%%%%%%%%%%%%%%%%%%%%%%%%%%%%%%%%%%%%%%%%%%%%%%%%%%%%%%%%%%%%%%%%%%%%%%%%
%
%     Set up default parameters
%
%%%%%%%%%%%%%%%%%%%%%%%%%%%%%%%%%%%%%%%%%%%%%%%%%%%%%%%%%%%%%%%%%%%%%%%%

fprintf('\n\n The default variables are:\n\n');
fprintf('Output error tolerance (sse) = 1\n');              tolerance = 50000;
fprintf('Errors plotted in progress every 10 epochs.\n');  epoch_disp = 10;
                                                  plotflag = 1;
fprintf('Maximum number of training epochs = 50.\n');      maxepochs = 50;



%%%%%%%%%%%%%%%%%%%%%%%%%%%%%%%%%%%%%%%%%%%%%%%%%%%%%%%%%%%%%%%%%%%%%%%%
%
%   Allow user to change default parameters
%
%%%%%%%%%%%%%%%%%%%%%%%%%%%%%%%%%%%%%%%%%%%%%%%%%%%%%%%%%%%%%%%%%%%%%%%%

choice = input('Are you satisfied with these selections? [y,n]:','s');

if choice == 'n'
epoch_disp = input('How often to display error(# of epoches): ');
tolerance = input('Output error tolerance (sse): ');
maxepochs = input('Maximum number of epoches to train: ');
end

%%%%%%%%%%%%%%%%%%%%%%%%%%%%%%%%%%%%%%%%%%%%%%%%%%%%%%%%%%%%%%%%%%%%%%%%
%
%        Load training data
%
%%%%%%%%%%%%%%%%%%%%%%%%%%%%%%%%%%%%%%%%%%%%%%%%%%%%%%%%%%%%%%%%%%%%%%%%

eval(['load ',vecfile])
```

```
[nov1,numin] = size(x);
[nov2,numout] = size(y);

if nov1~=nov2
 error('The number of input vectors and target vectors has to be the same.')
end
fprintf('\nThis network has:\n\n');
fprintf('%0.f input neurons\n',numin);
fprintf('%0.f neurons in the hidden layer\n',numhid);
fprintf('%0.f output neurons\n\n',numout);
fprintf('There are %0.f input/output pairs in this training set.\n\n',nov1);

%%%%%%%%%%%%%%%%%%%%%%%%%%%%%%%%%%%%%%%%%%%%%%%%%%%%%%%%%%%%%%%%%%%%%%%
%
%         Scale inputs
%
%%%%%%%%%%%%%%%%%%%%%%%%%%%%%%%%%%%%%%%%%%%%%%%%%%%%%%%%%%%%%%%%%%%%%%%

if sc=='m'
    [xn,xm,xs]=zscore(x);
elseif sc=='l'
    [xn,xm,xs]=scale(x);
else


    xn=x;
end

%%%%%%%%%%%%%%%%%%%%%%%%%%%%%%%%%%%%%%%%%%%%%%%%%%%%%%%%%%%%%%%%%%%%%%%
%
%       Initialize weight vectors to small values
%
%%%%%%%%%%%%%%%%%%%%%%%%%%%%%%%%%%%%%%%%%%%%%%%%%%%%%%%%%%%%%%%%%%%%%%%

[R,Q]=size(xn');
S1=numhid;
[S2,Q]=size(y');

[W1,B1]=rands(S1,R);
[W2,B2]=rands(S2,S1);
W2=W2*.5;
W1=W1*.5;
B2=B2*.5;
B1=B1*.5;

%%%%%%%%%%%%%%%%%%%%%%%%%%%%%%%%%%%%%%%%%%%%%%%%%%%%%%%%%%%%%%%%%%%%%%%
%
%        Set training parameters for Levenberg-Marquardt
%
%%%%%%%%%%%%%%%%%%%%%%%%%%%%%%%%%%%%%%%%%%%%%%%%%%%%%%%%%%%%%%%%%%%%%%%

TP=[epoch_disp,maxepochs,tolerance,.0001,.001,10,0.1,1e10];
```

```
if sel1 == 'l'          % First layer selection
    F1 = 'purelin';
elseif sel1 == 't'
    F1 = 'tansig';
else
    F1 = 'logsig';
end

if sel2=='t'            % Second layer selection
    F2 = 'tansig';
elseif sel2=='l'
    F2 = 'purelin';
else
    F2 = 'logsig';
end



%%%%%%%%%%%%%%%%%%%%%%%%%%%%%%%%%%%%%%%%%%%%%%%%%%%%%%%%%%%%%%%%%%%%
%
%          Train the network using LM
%
%%%%%%%%%%%%%%%%%%%%%%%%%%%%%%%%%%%%%%%%%%%%%%%%%%%%%%%%%%%%%%%%%%%%

[W1,B1,W2,B2,epochs,TRLM] = trainlm(W1,B1,F1,W2,B2,F2,xn',y',TP);

%%%%%%%%%%%%%%%%%%%%%%%%%%%%%%%%%%%%%%%%%%%%%%%%%%%%%%%%%%%%%%%%%%%%
%
%          LM tolerance criteria not met
%
%%%%%%%%%%%%%%%%%%%%%%%%%%%%%%%%%%%%%%%%%%%%%%%%%%%%%%%%%%%%%%%%%%%%

if epochs==maxepochs
      fprintf('\n\***LM training complete, no answer found!')
      fprintf('\n*** SSE=%e \n\n',min(TRLM))
else

%%%%%%%%%%%%%%%%%%%%%%%%%%%%%%%%%%%%%%%%%%%%%%%%%%%%%%%%%%%%%%%%%%%%
%
%          LM tolerance criteria met
%
%%%%%%%%%%%%%%%%%%%%%%%%%%%%%%%%%%%%%%%%%%%%%%%%%%%%%%%%%%%%%%%%%%%%

      fprintf('\n*** LM training complete after %0.f epochs! ***', epochs)
      fprintf('\n*** SSE = %e \n\n',min(TRLM))
end

save WEIGHTS W1 B1 W2 B2 xm xs F1 F2 sc

%END
```

VITA

Christopher Lee Whitten was born January 26, 1975 in Florence, Alabama. He grew up in Wayne County, Tennessee where he attended Collinwood Elementary School and graduated from Collinwood High School in May 1993.

The author entered The University of Tennessee, Martin in August 1993 and transferred to The University of Tennessee, Knoxville in August 1995. He received a Bachelor of Science Degree in Agricultural Engineering in May 1999. He entered The University of Tennessee Graduate School in August 1999. He received a Master of Science Degree in Biosystems Engineering in May 2002.